# Flash Flood Risk Assessment in Egypt

Ahmed M. Helmi and Omar Zohny

**Abstract**

The subject of the flash flood risk assessment is an inclusive task that relies on the characteristics of the study area and the nature of previously recorded incidents. The Egyptian Nile Wadies (East Nile, and West Nile) are draining toward the highest population density and associated assets, while the Red Sea and Sinai wadies are draining toward high-density touristic compounds and scattered big cities and connecting roads. The existence of high urban densities and associated assets in the highest discharge locations (at wadies outfalls) without adequate consideration of wadi paths led to a considerable wadies encroachments and catastrophic recorded incidents. All recorded incidents are either due to unplanned urban and agricultural expansion, or insufficient flood mitigation measures, or lack of maintenance. Due to the freshwater stress in Egypt, the rainfall harvesting in the form of dams or artificial lakes should be considered as a top priority flood mitigation measure wherever applicable. The total capacity of all flood protection dams and artificial lakes all over Egypt is about 70 million $m^3$ (MWRI 2016) that raises the potentiality for more similar measures to increase the rate of investment return from both flood mitigation and reduction in freshwater stress. The available data for this study were sufficient enough to calculate the catchments peak discharge and runoff volume. The 100 year return period was selected for the peak discharge calculations. Many thresholds have been tested for catchment delineation in order to obtain a reasonable number of catchments suitable for such a regional-scale study. The SRTM 90 × 90 DEM file was utilized as an input in the delineation procedure, with selected threshold was set to 50 $km^2$. Due to the large variance of the catchments peak discharge and runoff volume, the box plot technique was employed to eliminate the ranking outlier values. The catchments were classified into five categories very high risk, high risk, moderate risk, low to moderate risk, and low risk. This categorization was done for the Peak Flow Standardized Risk Factor (PFSRF) and Runoff Volume Standardized Risk Factor (RVSRF) in order to prioritize the flood mitigation measures required for projects. The classification based on the runoff volume can guide the designer accounting for rain harvesting projects that would increase the rate of investment return from both flood mitigation and the reduction of freshwater stress. A two-dimensional HEC-RAS rainfall-runoff modeling is conducted for Ras Gharib city by using updated 30 × 30 DEM files to contain the manmade topographical modifications. The model was verified versus aerial photos for the 2016 incident. In order to assess the effectiveness of the newly constructed culvert (16 vents, 3 m × 3 m box culvert) with attached two dikes, another updated two-dimensional HEC-RAS rainfall-runoff model has been conducted and the results showed significant improvement in flood intensity values in Ras-Gharib city.

**Keywords**

Peak flow • Runoff volume • Standardized risk factor • Stormwater harvesting • Freshwater stress

A. M. Helmi (✉)
Department of Irrigation and Hydraulics, Faculty of Engineering, Cairo University, Giza, P.O.Box 12613 Egypt
e-mail: ahmed.helmi@eng.cu.edu.eg

O. Zohny
AIEcon. Consultants, Cairo, Egypt


A. M. Negm (ed.), *Flash Floods in Egypt*, Advances in Science, Technology & Innovation,
https://doi.org/10.1007/978-3-030-29635-3_13

**Abbreviations and Notations**

| | |
|---|---|
| A | Catchment Area ($km^2$) |
| ASRF | Catchment Area Standardized Risk Factor |
| CN | Curve Number |
| $D$ | Rainfall duration corresponding to the time step of calculations |
| $D_d$ | Drainage density |
| $d$ | Flow depth |
| DSRF | Drainage Density Standardized Risk Factor |
| FI | Flood Intensity |
| $F_s$ | Stream frequency |
| FSRF | Drainage Frequency Standardized Risk Factor |
| GIS | Geographic Information System |
| IF | Intensity Factor |
| $L$ | Longest flow path in (m) |
| LSRF | Surface flow Length Standardized Risk Factor |
| MENA | The Middle East and North Africa |
| MWRI | Ministry of Water Resources and Irrigation |
| $N_u$ | Number of streams of order ($U$) |
| $N_{u+1}$ | Number of streams of order ($U$ + 1) |
| O&M | Operation and Maintenance |
| PFSRF | Peak Flow Standardized Risk Factor |
| $R_b$ | Bifurcation ratio |
| RVSRF | Runoff Volume Standardized Risk Factor |
| $S_l$ | Slope of the longest flow path |
| SRTM | Shuttle Radar Topography Mission |
| SSRF | Slope Standardized Risk Factor |
| TCSRF | Time of Concentration Standardized Risk Factor |
| $T_c$ | Time of concentration in (min) |
| $T_L$ | Lag time |
| $T_p$ | Time to peak discharge |
| $TL_s$ | Total length of streams (m) |
| $TN_s$ | Total number of streams |
| $U$ | Stream orders according to (Horton 1945) |
| $V$ | Flow Velocity |
| WSRF | Weighted Standardized Risk Factor |
| WMO | World Meteorological Organization |

## 1 Introduction

Flash floods are natural phenomenon characterized by its short duration and massive runoff volume with limited time for response. As a natural phenomenon, flash floods depend on climatic conditions, geological nature, and prevailing terrain. The rainfall in Egypt starts at the beginning of the fall season as of mid-October. Falling rains on mountains and large catchment form streams with high velocity in case of the topographical high slopes, carrying sedimentary materials and stones located on the soil surface and leading to severe damage to the assets located at the catchments outlets. In Egypt, the highest population density is centralized around the Nile banks and high-density touristic compounds and scattered big cities with connecting roads are distributed along the whole Red Sea coast, and in the Sinai Peninsula. The high-density urbanization with all associated assets without proper consideration of wadi paths led to a considerable wadies encroachment and catastrophic recorded incidents.

Due to the huge amount and the cost of work required for encroachments assessment and the implementation of proper flood mitigation measures, prioritization of wadies based on its Peak Flow Standardized Risk Factor (PFSRF) has been a critical task since most of the encroachments are located at wadies outlets. Stormwater harvesting can provide a share in reducing freshwater stress associated with a reduction in the required drainage structures accordingly, another catchments prioritization is provided based on Runoff Volume Standardized Risk Factor (RVSRF). The provided RVSRF can guide the designer to give a priority for artificial lakes and dams as a recommended flood mitigation measure for such catchments. The storage capacity of all flood mitigation measures in Egypt is about around 70 million $m^3$ (MWRI 2016), which raises the potentiality to increase the number of similar flood mitigation measures.

For future planning, 30 × 30 DEM files, and two-dimensional Rainfall-Runoff HEC-RAS can be a useful tool for performing an initial assessment of flood plain. However, this does not replace the topographic survey at project location with reasonable coverage of the surroundings to capture fine terrain details that cannot be achieved by using DEM files, especially in flat terrain areas.

## 2 The Study Area

Egypt is divided into six hydrological regions based on its hydrological parameters and outfalls.

- Sinai hydrological region.
- Nile hydrological region.
- Red Sea hydrological region.
- Northern coast hydrological region.
- Delta hydrological region.
- Oasis hydrological region.

The study area covers the Nile, Red Sea, and Sinai hydrological regions. The catchments outlets are endangering densely populated areas, as shown in Fig. 1.

## 3 Flash Flood Characteristics

Flash flood is a natural phenomenon that has a variety of definitions. The WMO states that a flash flood is: "A flood of short duration with a relatively high peak discharge." The American Meteorological Society (AMS) defines flash floods as "A flood that rises and falls quite rapidly with little or no advance warning, usually as the result of intense rainfall over a relatively small area." In terms of warnings, a flash flood is a local hydrometeorological phenomenon that requires: Both Hydrological and Meteorological expertise in real-time forecasting/warning and knowledge of local, up to the hour information for effective warning (24/7 operation). Response time to flash floods is usually less than 6 h (WMO 2012).

The flash flood discharge at the catchment outlet is affected by the rainfall (intensity, duration, distribution, and directions), catchment properties (shape, average slope, stream slope, soil infiltration rate, and the existence of surface depression) as shown in Fig. 2. The danger of flash floods is due to its sudden occurrence associated with a large flow velocity which moves large amounts of debris and sediments. The force of the flow can be high enough to destroy structures and buildings that stand in its path. A flash flood may also result from a failure of dams, embankments, or other hydraulic infrastructures, and when it is associated with a storm event it dramatically increases its negative impacts.

## 4 Flood Risk Assessment

Definition of flash flood risk is a mandatory step prior to the flood management planning stage. The risk is the potential losses that can occur due to any disaster. In the case of flood, it indicates the impact of a flash flood on human lives, environment, and properties. Three crucial elements are required to characterize the flash flood risks (hazards, exposure, and vulnerability), as shown in Fig. 3. For flash flood consideration the three items can be defined as follows:

**Hazard**: can be defined as the "flood inundation maps showing the depths of inundation and related water velocities for a storm event corresponding to an agreed return period." The risk assessment of human lives and assets will be properly defined after considering the exposure and vulnerability parameters. The hazard also can be defined as the value of the discharge or volume of runoff as the parameters used to rank the catchments regarding the risk at its outlets and the potential of stormwater harvesting.
**Exposure**: can be defined as "people, properties, infrastructure, housing, and any other type of assets located in a predefined hazard area." The exposure can be presented in land-use maps, infrastructure maps, population density maps, etc.
**Vulnerability**: can be defined as "The risk scale determination of an individual, a community, and assets to the impacts of flood hazard" which can be defined by considering the health, physical, social, and economic conditions of the considered items in the hazard area. It can be presented in a map with, the very low, low, medium, high, and very high-risk scale for each considered item.

The water resources in Egypt as in all Middle East and North Africa (MENA) Region are subjected to high stresses due to the population increase, which requires that the flood mitigation measures are not only for protection purpose, but also it has to consider a proper utilization of this freshwater. "That is why it would be of little use to consider Flood Risk Assessment (FRA) by itself without casting it in the framework of flood risk management and water management at large," (Rudari 2017).

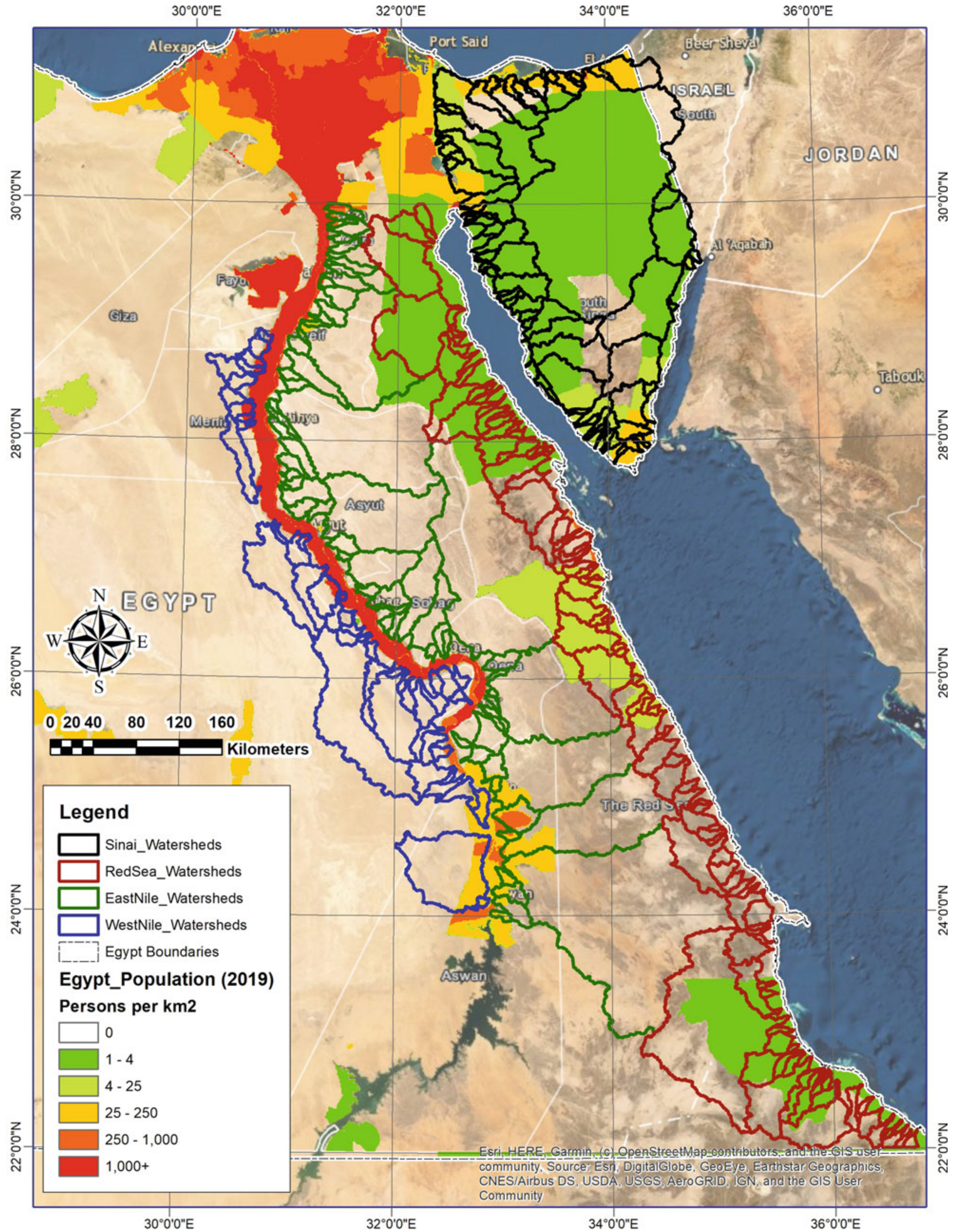


**Fig. 1** Distribution of population densities. Adapted from NASA (2019)

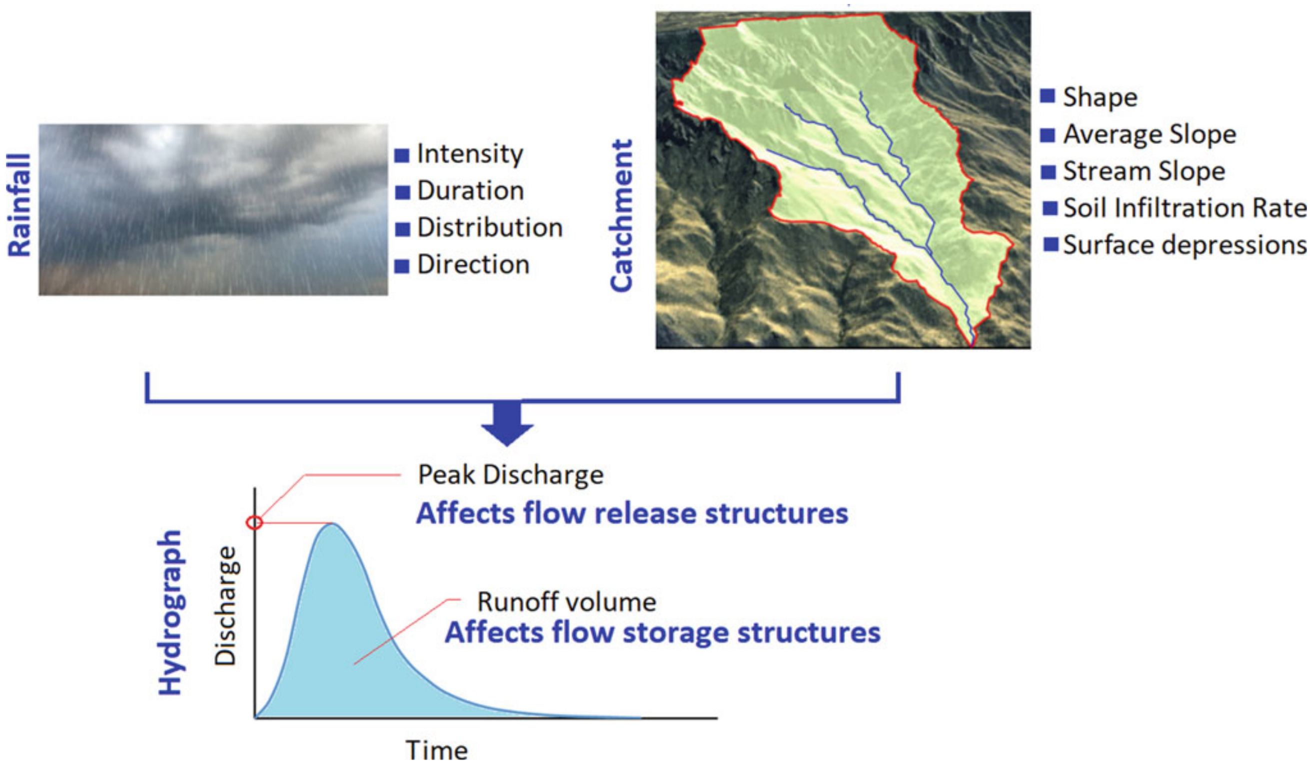


**Fig. 2** Factors affecting catchments' outlet hydrographs

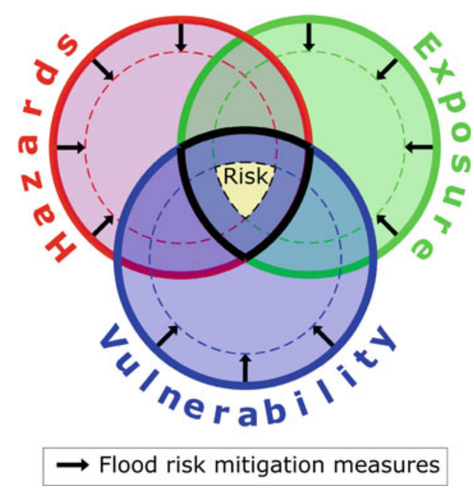


**Fig. 3** Flood risk characterization. Adapted from WMO (2006)

High-resolution flood inundation maps are costly and require a very detailed topographical data, and intensive calibration works. It is recommended to divide the procedure of obtaining Flood Risk Plan (FRP) into two stages:

**Preliminary Flood Risk Assessment (PFRA)**: which is utilized to define priority areas using Digital Elevation Models (DEMs), brake lines, and available flood mitigation measures for further detailed assessment.

**Final detailed Flood Risk Assessment (FRA)**: to be applied to the high-risk areas defined in the PFRA in order to maximize the return on investment where many more resources are invested in the topographical survey, modeling, and calibration. The potential areas of development should be taken into consideration, although they have not been shown in preliminary studies (European-Commission 2016).

In addition to the previous procedure, the historical information is an extremely important source of information from the flash flood that has occurred in the past, and its impacts for a specific event is a fact with 100 % confidence.

## 5 Sample of Previous Flash Flood Incidents

On Friday, October 28, 2016, seven people were killed and 23 others injured after heavy rain hit Ras-Gharib city in the Red Sea governorate as shown in Fig. 4. The main cause of this catastrophic incident was not due to the rainfall depth on Ras-Gharib city; instead, it was due to the diversion of almost 70 % of wadi Had catchment flow toward the city. The diversion of wadi from its natural stream path toward the city was due to the missing drainage structures along Ras-Gharib–El-Sheikh-Fadl road, as shown in Fig. 5. The proposed solution was to provide access to allow the wadi to

**Fig. 4** Ras-Gharib incident destructive flood impacts (2016)

restore back to its natural path (16 vents 3 m × 3 m culvert) along with two dikes to ensure the complete flow guidance to the original wadi path, as shown in Fig. 6.

On Tuesday, June 17, 2010, Aswan Governorate witnessed a flood event that swept the home furnishings and people, leaving behind many houses destructions in addition to the damage to thousands of feddans of agricultural land, as well as damaging tons of harvested dates which people had put them under the sun to dry out as shown in Fig. 7. Although the wadi was provided by two dikes to guide the flow toward the drainage channel leading to the River Nile as shown in

Figure 8 due to the lack of maintenance and the use of the channel as a dump site and drain to the houses and agricultural land, the capacity of the drainage channel was reduced and led to the occurred flooding negative impacts (Figs. 9 and 10).

Frequent occurring incidents affect rural roads due to insufficient flood protection measures.

## 6 General Investigations of Flash Flood Triggers in Egypt

As a global view and according to the collected data from stakeholders, the main causes of flash flood problems can be summarized in the following points:

1. The global warming accelerates the water and led to an intensification of the rainfall (Syed et al. 2010). There is evidence of increased frequency and severity of flash flooding in recent years (USAID 2018).
2. Flood plain encroachment (Wadi Degla, Red sea coast, Wadi Al Khurait). A sample is shown in Fig. 11.
3. Due to the high rates of encroachment on the floodways and the difficulty of determining the current flood path from digital elevation models or maps as shown in Fig. 12. It is necessary to update aerial-photogrammetry of the wadies downstream areas.
4. Excessive urbanization in the vicinity of major roads leading to a reduction in soil infiltration and increase in flood peak discharges will be catastrophic if no attenuation structures will be provided to ensure that the existing flood mitigation measures will safely operate as shown in Figs. 13 and 14. A sample of an artificial pond is located at Madinaty, as shown in Fig. 15.
5. Some major roads passing through wadies without any drainage structures to allow the flow in its natural path, leading to the diversion of wadi paths toward urbanized areas (Ras Gharib–El-Sheikh-Fadl road) as shown in Figs. 5 and 6.
6. There are encroachments by the people on the dam sites and the theft of some dam materials (stones and gabions), which caused the collapse of some dams (Al Ain-Al Sukhna Dams).

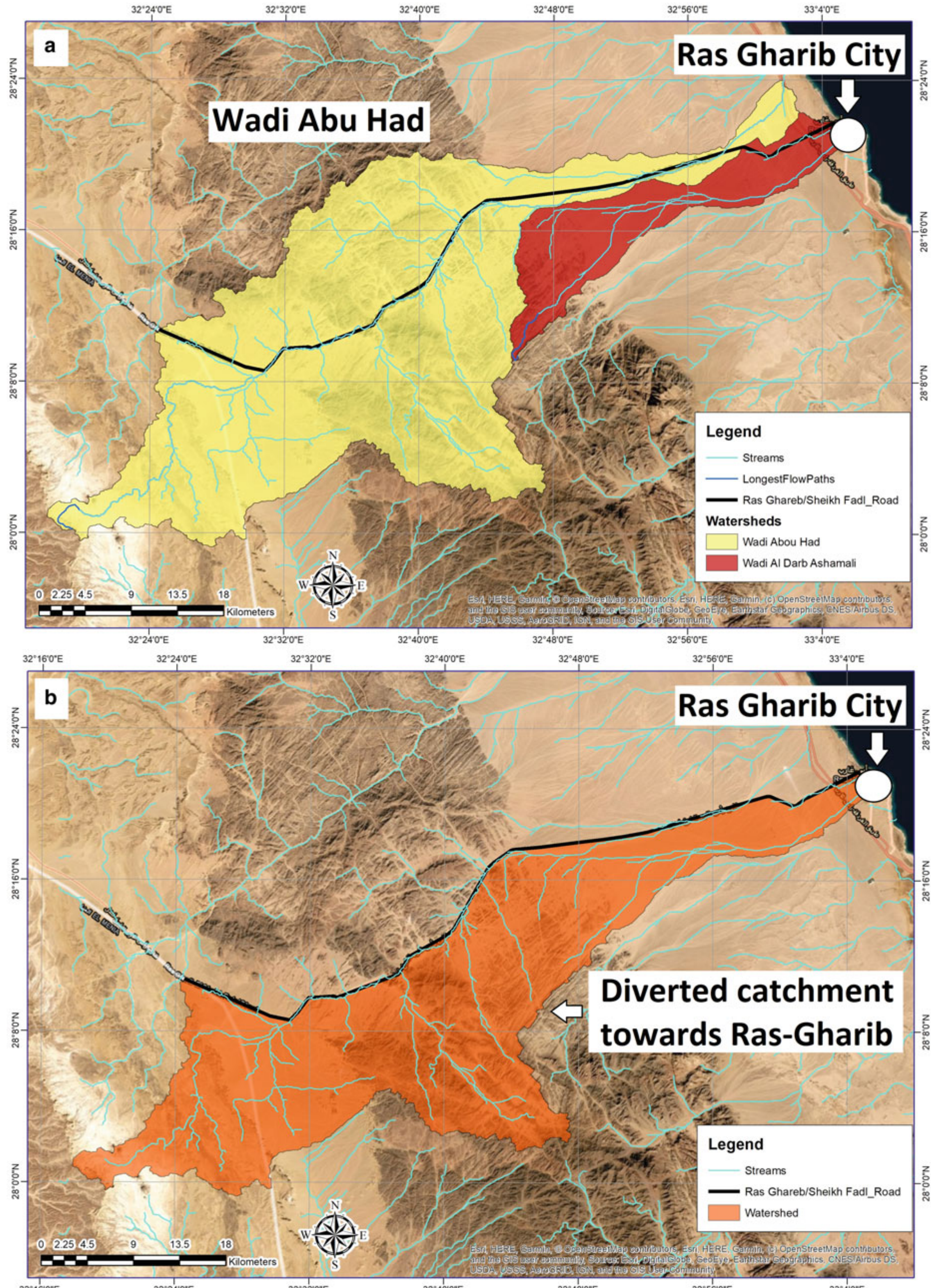


**Fig. 5** Catchments attacking Ras-Gharib City, **a** initial conditions; **b** after elevating Ras-Gharib–El-Sheikh-Fadl road

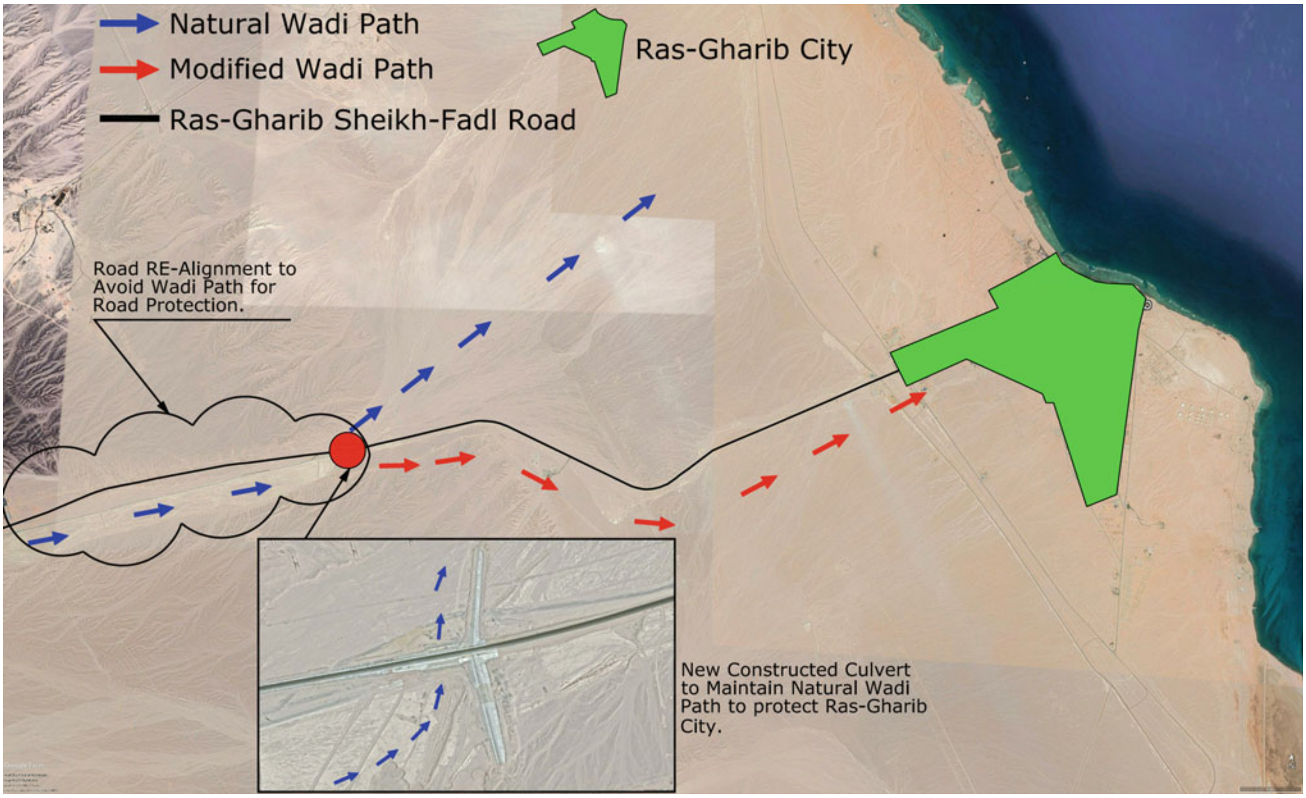


**Fig. 6** Flood mitigation measures after Ras-Gharib 2016 incident

**Fig. 7** Buildings are destroyed in Abouelreesh village in Aswan governorate after a torrent on June 17, 2010

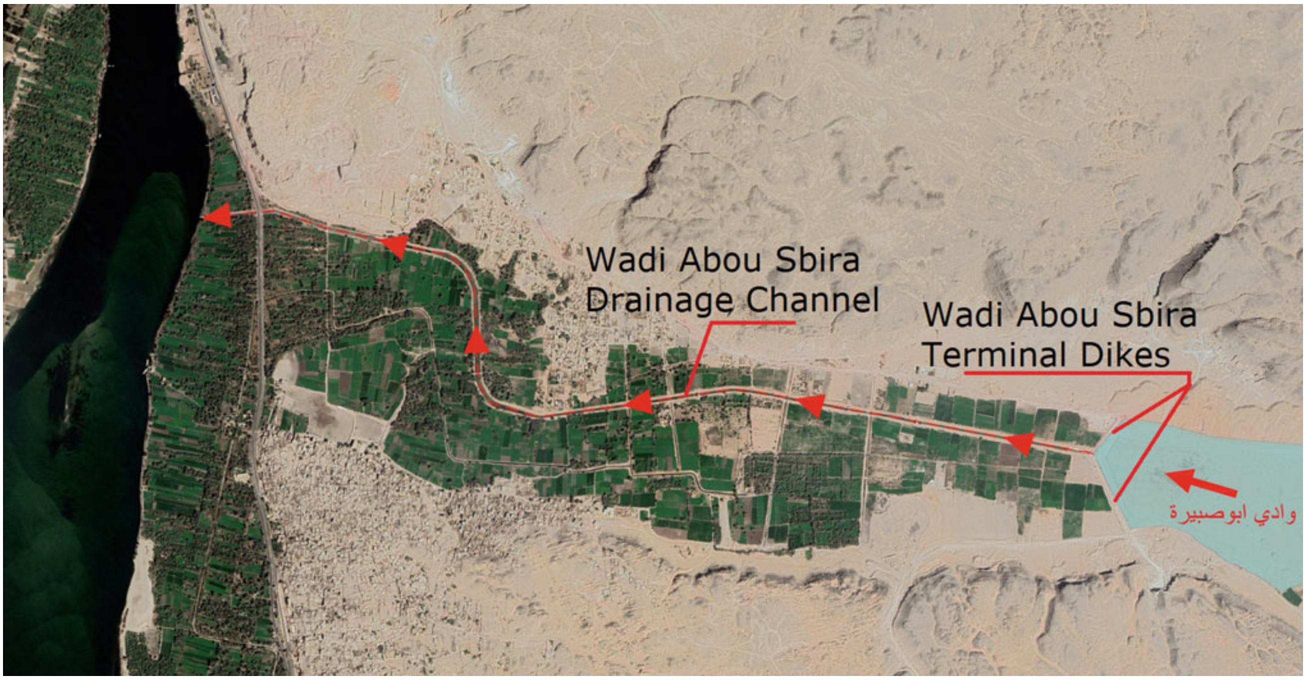


**Fig. 8** Wadi Sbira drainage system toward the Nile

**Fig. 9** El Sokhna road during April 25, 2018 rains, 2018

**Fig. 10** Safaga-Qina road after April 12, 2017 rains

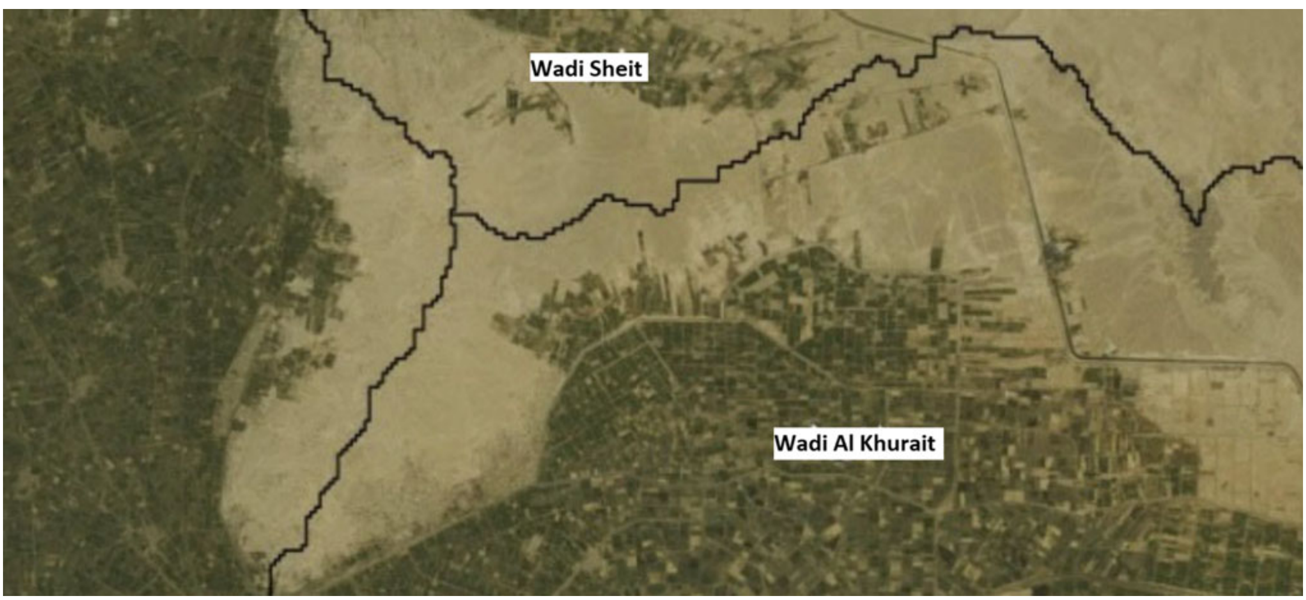


**Fig. 11** Wadi Al Khurait encroachments at Aswan governorate (MWRI 2016)

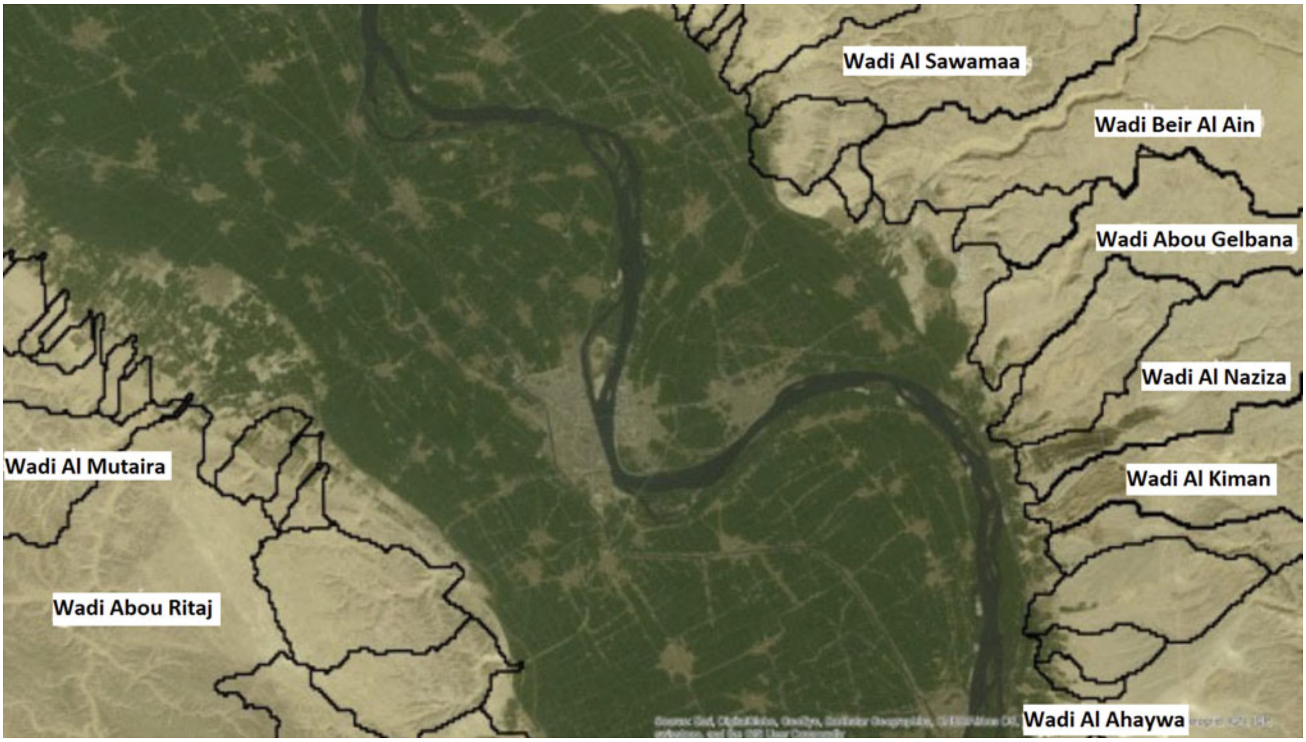


**Fig. 12** Lost stream paths due to the expansion of urban areas and agricultural lands (MWRI 2016)

**Fig. 13** Fifth settlement flooding (Helmi et al. 2019)

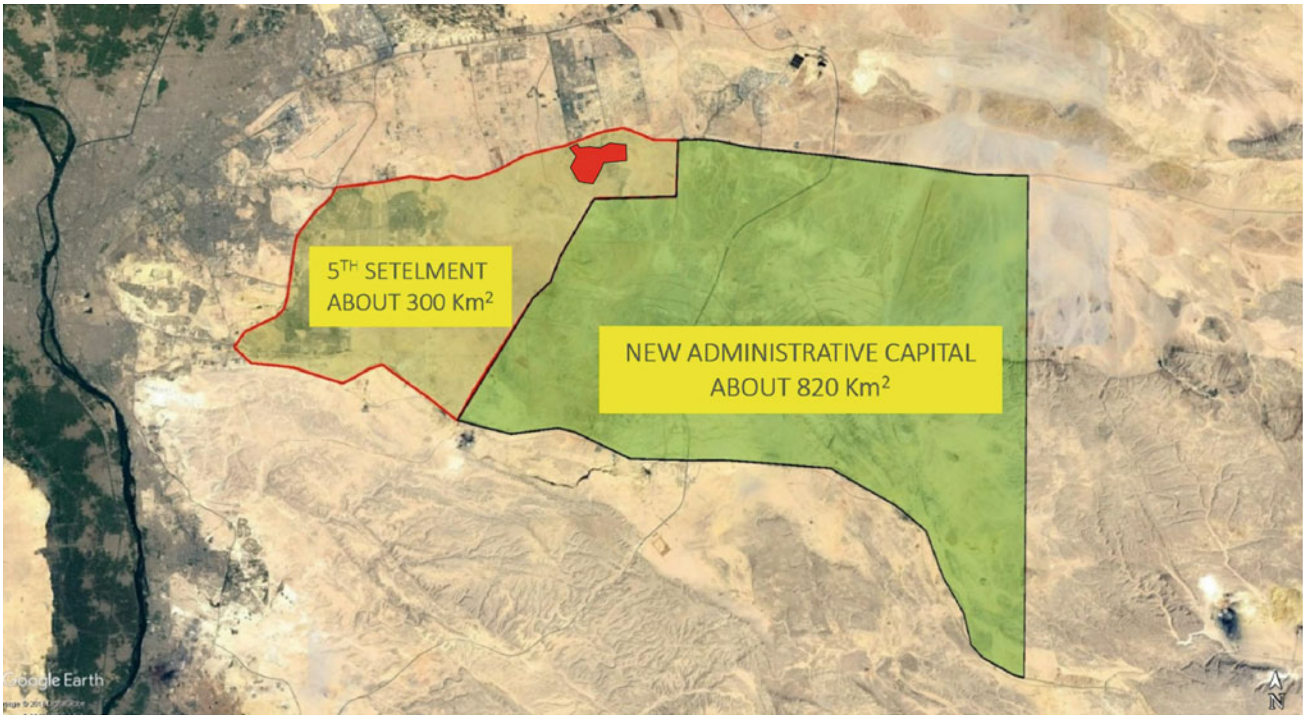


**Fig. 14** Excessive urbanization at the southern side of Suez Road, (Helmi et al. 2019)


**Fig. 15** Madinaty channelized wadi with four vents entrance culverts draining to a smaller culvert under Suez road and temporary detention pond

**Fig. 16** Partial failure of Galawya dam due to the use of the dam top as an access road for quarries trucks (MWRI 2016)

7. The use of the top of the dams as access roads for the quarries to provide an easier path for heavy trucks as the case of (Galawiya Dam-Sohag Governorate) shown in Fig. 16.
8. There is no detailed storm drainage and flood mitigation design code to be used as a unified reference for all studies.
9. The high cost, and lengthy process of collecting rainfall data from the General Meteorological Authority even for universities and research institutes.
10. Many entities are responsible for projects affecting and/or affected by the wadies paths without any coordination with the main bodies responsible for these studies.

## 7 Risk Assessment of Flash Floods in Egypt

Many previous studies focused on the flash floods risk assessment in Egypt can be found in the literature. The majority of the articles relies on the catchments morphological characteristic and some studies considered the catchment discharge

(El-Shamy 1992) proposed a simple morphometric method to estimate the flash flood risk levels and the degree of hazardousness for each subbasin. Two different approaches were elaborated to determine hazardous sub-watersheds. The first is based on the relationship between bifurcation ration $(R_b)$ and drainage density $(D_d)$, whereas the second approach utilized the relationship between bifurcation ratio $(R_b)$ and stream frequency $(F_s)$ as given in Fig. 17. Drainage density $(D_d)$ refers to topographic dissection, runoff potential, infiltration capacity of surface materials, climate, and land cover of the watershed. In this regard, low values of $(D_d)$ indicate optimal conditions for infiltration, thus decreasing runoff potential, while high stream frequency $(F_s)$ represents impermeable sub-surface materials, poor vegetation cover, high relief, and low infiltration capacity, hence increasing runoff potential. Applying this relationship separately to each subbasin will provide reasonable information on the estimation of flooding risk and recharge potential. In order to assess such relations, three morphometric parameters $(R_b, D_d, \text{and } F_s)$ must be calculated for each subbasin (Al-Saud 2010).

$$F_s = \frac{\mathrm{TN}_s}{A} \tag{1}$$

$$D_d = \frac{\mathrm{TL}_s}{A} \tag{2}$$

$$R_b = \frac{N_u}{N_{u+1}} \tag{3}$$

where

| | |
|---|---|
| $\mathrm{TN}_s$ | Total number of streams. |
| $\mathrm{TL}_s$ | Total length of streams (m). |
| $A$ | Catchment Area ($km^2$). |
| $U$ | Stream orders according to (Horton 1945). |
| $N_u$ | Number of streams of order ($U$). |
| $N_{u+1}$ | Number of streams of order ($U$ + 1). |

Eman et al. (2002) evaluated the morphometric parameters of Wadi Um-Harika attacking Mersa Alam and the connecting road to and from DEM files. The data was used to define flash flood-vulnerable sites along the Idfo-Marsa Alam road.

El-rayes and Omran (2009) estimated the flood risks of Wadi Hagul basin. They concluded that three subbasins out of Wadi Hagul basin are recognized as risky flooding areas. The resulted runoff due to rainfall storm depth of 49.6 mm event occurred in October 1965 and reached about 7.2 million $m^3$.

**Fig. 17** Flooding possibilities based on (El-Shamy 1992) model

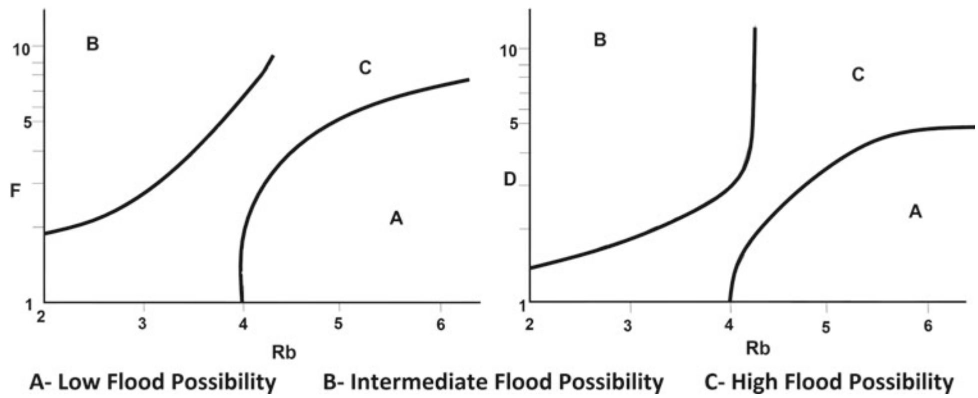


A multi-criteria standardized risk factors considering the (ASRF), (SSRF), (TCSRF), and Runoff Volume Risk Factor (RVSRF) was utilized by (El-moustafa 2012) to prioritize the flood protection work areas along Assiut Safaga Road in the eastern desert. Equal weight of each standardized risk factor was used to calculate (WSRF) to assess the risk of each catchment.

Mona Mohamed (2013) utilized multi-criteria analysis to assess the impact of morphological parameters on the risk categorization of some catchments located in the eastern desert and draining toward the Red Sea. The studied parameters were catchment Area Standardized Risk Factor (ASRF), Slope Standardized Risk Factor (SSRF), drainage Frequency Standardized Risk Factor (FSRF), drainage Density Standardized Risk Factor (DSRF), surface flow Length Standardized Risk Factor (LSRF), and Time of Concentration Standardized Risk Factor (TCSRF). The weight of each morphological factor was evaluated based on the impact on its peak flow discharges in order to obtain a Weighted Standardized Risk Factor (WSRF) that represents the equivalent catchment risk factor. As per the achieved weight of each risk factor, it was concluded that the (ASRF), (SSRF), and (TCSRF) are the most influential parameters affecting peak discharge.

Zaid et al. (2013) analyzed the flash flood of Wadi Abu-Hasah on Tall El-Amarna archeological area using GIS and Remote Sensing. They utilized (El-Shamy 1992) model to assess the flash flood hazard based on the morphological parameters, and concluded that the basin ranked as moderate to high hazard. They proposed a diversion channel to collect the surface water runoff away from the threatened, in addition to the construction of a dike around the tomb in order to minimize the water seeps into the tomb throughout the fractures and joints of the limestone section.

Abdel-fattah et al. (2017) investigated the relationship between variations in geomorphometric and rainfall characteristics and the responses of wadi flash floods. An integrated approach was developed based on geomorphometric analysis and hydrological modeling for Wadi Qina. Thirty-eight geomorphometric parameters representing the topographic, scale, shape, and drainage characteristics of the basins were considered and extracted using Geographic Information System (GIS) techniques. The results exhibited strong correlations between scale and topographic parameters and the hydrological indices of the wadi flash floods, while the shape and drainage network metrics have smaller impacts. The total rainfall amount and duration significantly impact the relationship between the hydrologic response of the Wadi and its geomorphometry.

Abdalla et al. (2014) utilized GIS-based morphometry and satellite imagery data to assess the flash floods occurrence and groundwater aquifers recharge relationship for Wadi El-Gemal, Wadi Umm El-Abas, Wadi Abu Ghuson, and Wadi Lahmi, along the southeastern Red Sea Coast in Egypt. The authors divided the studied areas into 45 subbasins and used (El-Shamy 1992) model to assess the potential for flash floods and groundwater recharge. Only two subbasins indicated the low potential of flooding and high potential of groundwater aquifers.

Elsadek et al. (2018) assessed the susceptibility of Wadi Qina watershed sub-catchments based on morphological parameters according to (El-Shamy 1992). The results illustrate that there are no subbasins with low risk of flooding. The subbasins with the highest hazard degree are concentrated in the middle of the watershed, although they have smaller areas compared with the surrounding subbasins. The subbasins located at the boundary of the watershed have an intermediate risk of flooding and moderate potential for groundwater recharge.

The Egyptian Ministry of Water Resources and Irrigation with cooperation with the National Water Research Center and Water Resources Research Institute published flood atlases for Aswan, Luxor, Qina, Assiut, Sohag, and North Sinai governorates while the Red Sea governorate is still under preparation. The risk assessment can be done by two approaches:

- Streamflow intensity: by evaluating the Intensity Factor (IF) obtained from multiplying the stream depth by the stream velocity at the catchments outlets. The results were classified into four ranges (low, medium, high, and high) for (IF) <1, 1–3, 3–5, and >5, respectively.
- Catchments Risk Assessment: by considering the catchment slope, Curve Number (CN), and 1-in-100 years' storm event as a governing factor in the determination of the catchment risk. The results were classified into four ranges (low risk, medium risk, high risk, and very high risk). No details were provided for the methodology used to achieve this classification.

In MWRI atlases the assessment is based on provincial boundaries and not a regional scale.

### 7.1 Available Data for the Study Area

Figure 18 shows the distribution of some of the Egyptian meteorological authority station, the 1-in-100 maximum daily precipitation in (mm) was collected from previous reports and studies for some meteorological stations located in the study area is given in Table 1. The 1-in-100 maximum daily precipitation is used to generate the isohyetal map for the study area as shown in Fig. 19. The 1:250000 topo map has been acquired, and georeferenced, to cover the study area as shown in Fig. 20. The regional SCS Curve Number (CN) is shown in Fig. 21 (Awadallah et al. 2016). The SRTM 90 × 90 DEM data has been collected and clipped to cover the study area as shown in Fig. 22.

### 7.2 Assessment of Previous Studies and Available Data

The available data in the study area can be utilized to obtain the catchment boundaries and streamlines from the DEM file for further verification versus the streamlines and wadies names available on topo maps. After the verification versus the topo maps, the morphological characteristics can be obtained for each catchment. The weighted average SCS CN for each catchment can be extracted using the GIS tool for each catchment. The GIS is utilized to produce an isohyetal map of the study area to obtain weighted 1-in-100 weighted average maximum daily precipitation for each catchment. Finally, each catchment peak 1-in-100 discharge and storm volume can be calculated. The proposed framework is summarized in Fig. 23 flow chart.

Most of the previous studies considered only the morphological parameters of the catchments in their weighted value or considered equal weigh morphological parameters and adding the volume of runoff as an additional parameter with the same weight. As well, all previous studies covered scattered parts of the eastern desert and no regional study was provided.

In this report, as long as the data collected are sufficient to calculate the runoff peak discharge, it will be used in its standardized value as an evaluating risk factor for the catchments. The Peak Flow Standardized Risk Factor (PFSRF) internally contains the morphological, geological, and meteorological parameters in their weighted form. PFSRF will be used to categorize the catchments based on their risk. The Runoff Volume Standardized Risk Factor (RVSRF) will be utilized in further catchments risk categorization, which will show the stormwater harvesting potential in addition to the risk generated if no proper flood mitigation measures are provided.

$$\text{Peak Flow Standardized Risk Factor (PFSRF)} = \frac{\text{PF} - \text{PF}_{\min}}{\text{PF}_{\max} - \text{PF}_{\min}} \quad (4)$$

$$\text{Runoff Volume Standardized Risk Factor (RVSRF)} = \frac{\text{RV} - \text{RV}_{\min}}{\text{RV}_{\max} - \text{RV}_{\min}} \quad (5)$$

The selected normalized ranges to classify the risk categories are given in Table 2.

### 7.3 Catchments Delineation

Many thresholds have been tested for catchments delineation in order to obtain a reasonable number of catchments for this regional-scale study. The selected threshold was set to 50 $km^2$.

### 7.4 Runoff Calculations

HEC-HMS software is used to calculate the catchment peak discharge and total volume of runoff. The selected calculation algorithm is the Soil Conservation Service SCS Curve Number method (USDA1986), where

$$R = \frac{(P - I_a)^2}{(P - I_a) + S} \quad (6)$$

$$S = \frac{25400}{\text{CN}} - 254 \quad (7)$$

where

$R$ Excess Runoff (mm).
$P$ Rainfall in (mm).


**Fig. 18** Distribution of Egyptian meteorological authority stations

**Table 1** Available rainfall stations frequency analysis results

| Name | Lat | Long | 1-in-100 Precipitation (mm) |
|---|---|---|---|
| Katamya | 30.07° | 31.83° | 21.4 |
| Sohag | 26.57° | 31.70° | 34.8 |
| Qina | 26.18° | 32.73° | 61.7 |
| Luxor | 25.67° | 32.70° | 39.6 |
| Komombo | 24.48° | 32.93° | 43.7 |
| Aswan | 23.97° | 32.78° | 25.4 |
| Helwan | 29.87° | 31.33° | 57.6 |
| Giza | 30.03° | 31.22° | 23.3 |
| Assyout | 27.05° | 31.02° | 66.4 |
| Suez | 29.87° | 32.47° | 49.6 |
| Hurghada | 27.28° | 33.77° | 81.4 |
| Quseir | 26.13° | 34.30° | 76 |
| Ras Banas | 23.97° | 35.50° | 81.4 |
| Sharm El-Sheikh | 27.96° | 34.30° | 50 |
| Abou Rdais | 28.91° | 33.19° | 58 |
| Nowebaa | 28.98° | 34.68° | 47 |
| Ras Sudr | 29.58° | 32.71° | 46 |
| Saint Catherin | 28.68° | 34.06° | 87 |
| Al Temed | 29.40° | 34.17° | 107 |

$S$ Potential maximum retention after runoff begins in (mm).

$I_a$ Initial abstraction in (mm)

$$I_a = 0.2S \tag{8}$$

6-h storm duration with SCS type II distribution, given in Fig. 24, was selected for hydrologic modeling of the catchments.

The time of concentration is among the different parameters which are used to identify the response of any given watershed to a rainfall storm event. Time of concentration is defined as the time required by a water drop to travel from the hydraulically most distant point of any given watershed to the watershed outlet (Ramirez 2000; Durrans 2007), the hydraulically most distant point is the point with the longest travel time. There are various empirical formulas to estimate the time of concentration from topographic and/or rainfall characteristics. The well-known Kirpich equation was originally developed based on SCS data from seven rural watersheds on a farm in Tennessee, these watersheds were characterized by well-defined channels, and steep slopes and their catchment areas were ranging from 1.25 to 112 acres (0.005–0.45 km$^2$).

The Kirpich formula can be expressed as follows:

$$T_c = 0.019472 \frac{L^{0.77}}{S_l^{0.385}} \tag{9}$$

where

$T_c$ Time of concentration in (min).

$L$ Longest flow path in (m).

$S_l$ Slope of the longest flow path.

The formula has been updated after (Rossmiller 1980) to consider the effect of CN

$$T_{c-\text{modified}} = T_c \times (1 + (80 - \text{CN}) * 0.04) \tag{10}$$

The Unit Hydrograph (UH) is the actual response of any given watershed (in terms of runoff volume and timing) to a unit input of excess rainfall. First proposed by (Sherman 1932), it can be defined as the Direct Runoff Hydrograph (DRH) resulting from one unit (e.g., one cm or one inch) of excess rainfall occurring uniformly over a watershed at a uniform rate over a unit time (Sherman 1941; Chow 1959; Ramirez 2000; Weaver 2003). The SCS dimensionless unit hydrograph given in Fig. 25 is used in the hydrologic simulation for the case in hand.

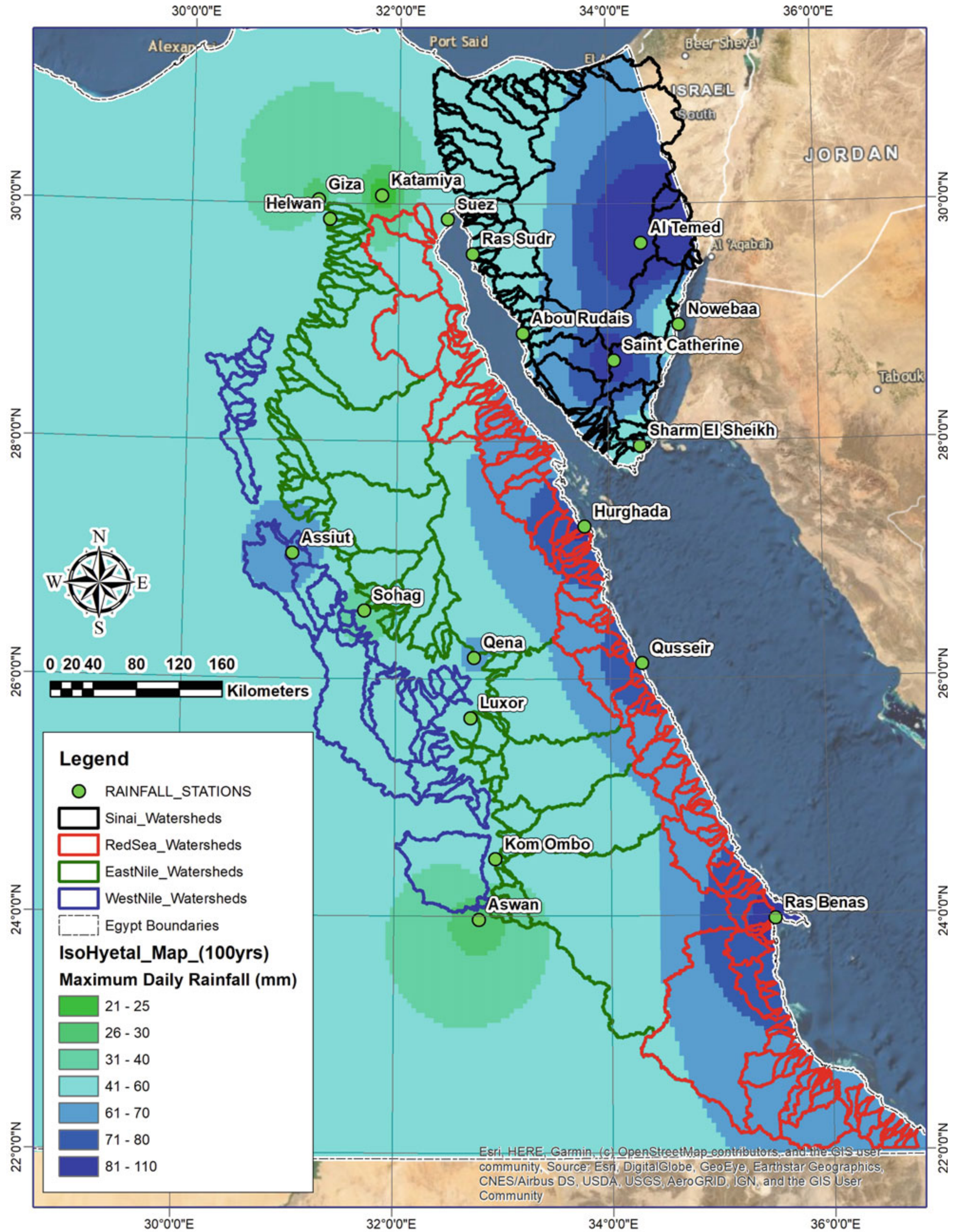


**Fig. 19** Isohyetal map for the study area

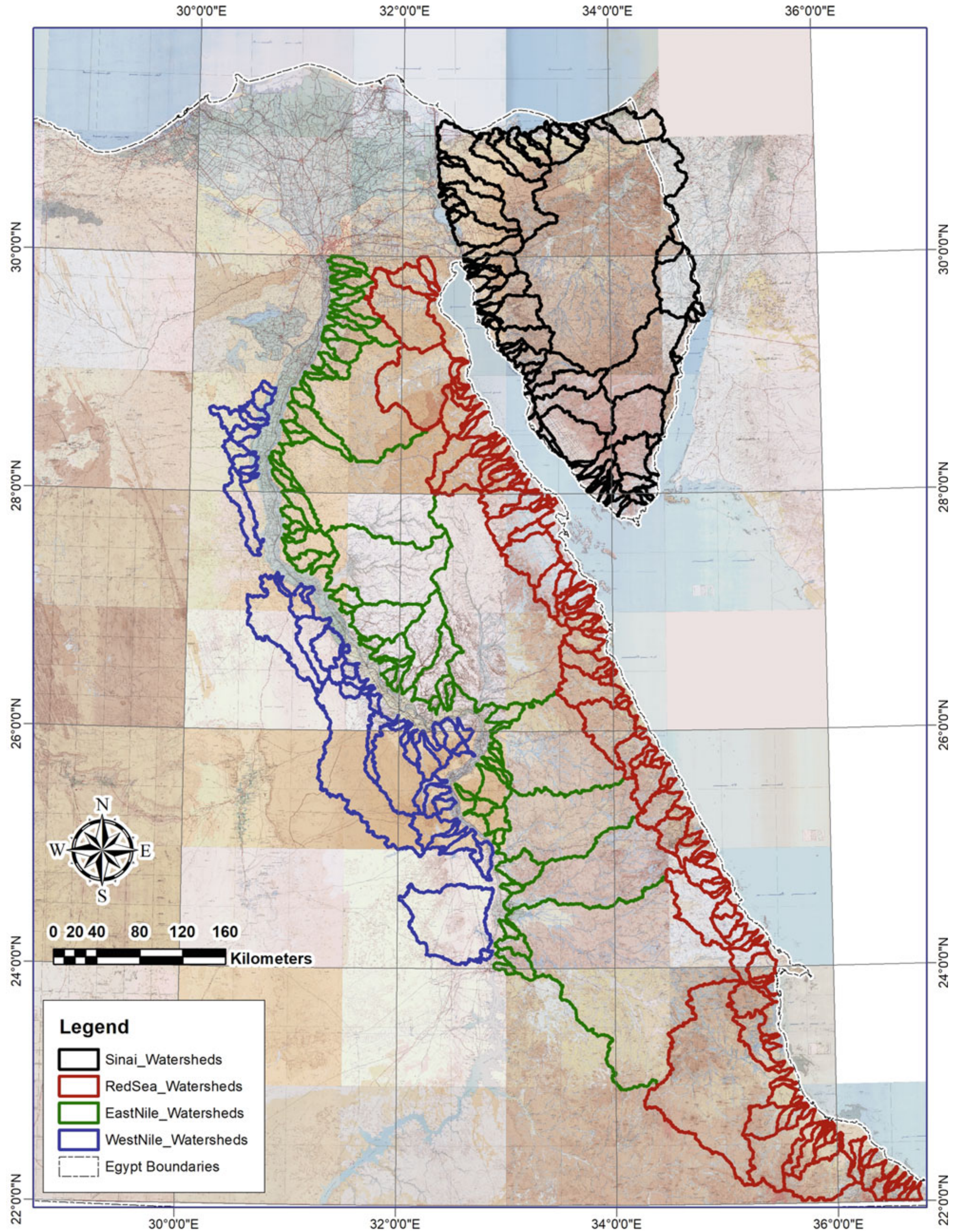


**Fig. 20** The study area on topo maps (Scale 1:250,000)

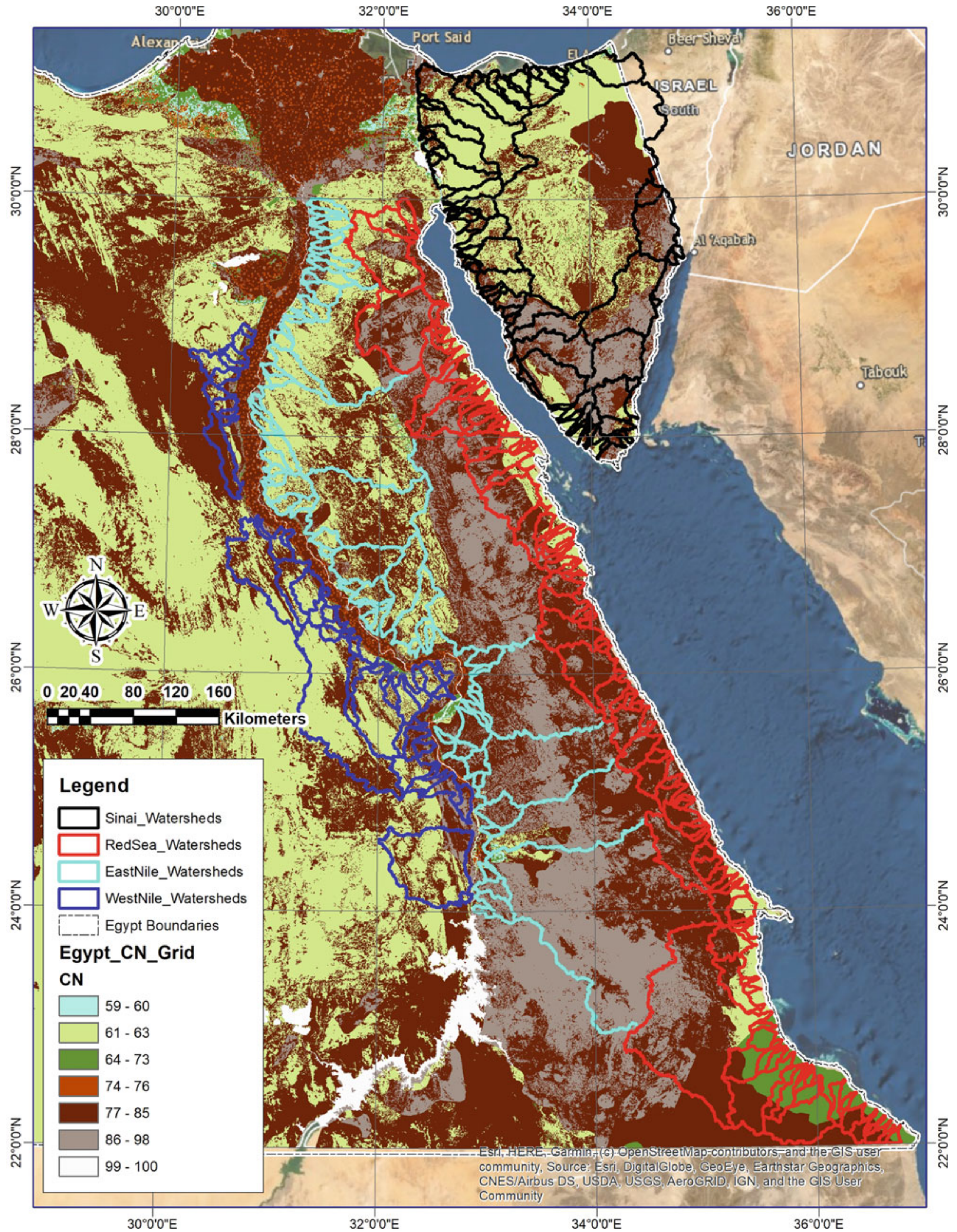


**Fig. 21** The study area on regional SCS Curve Number (CN) for Egypt (Awadallah et al. 2016)

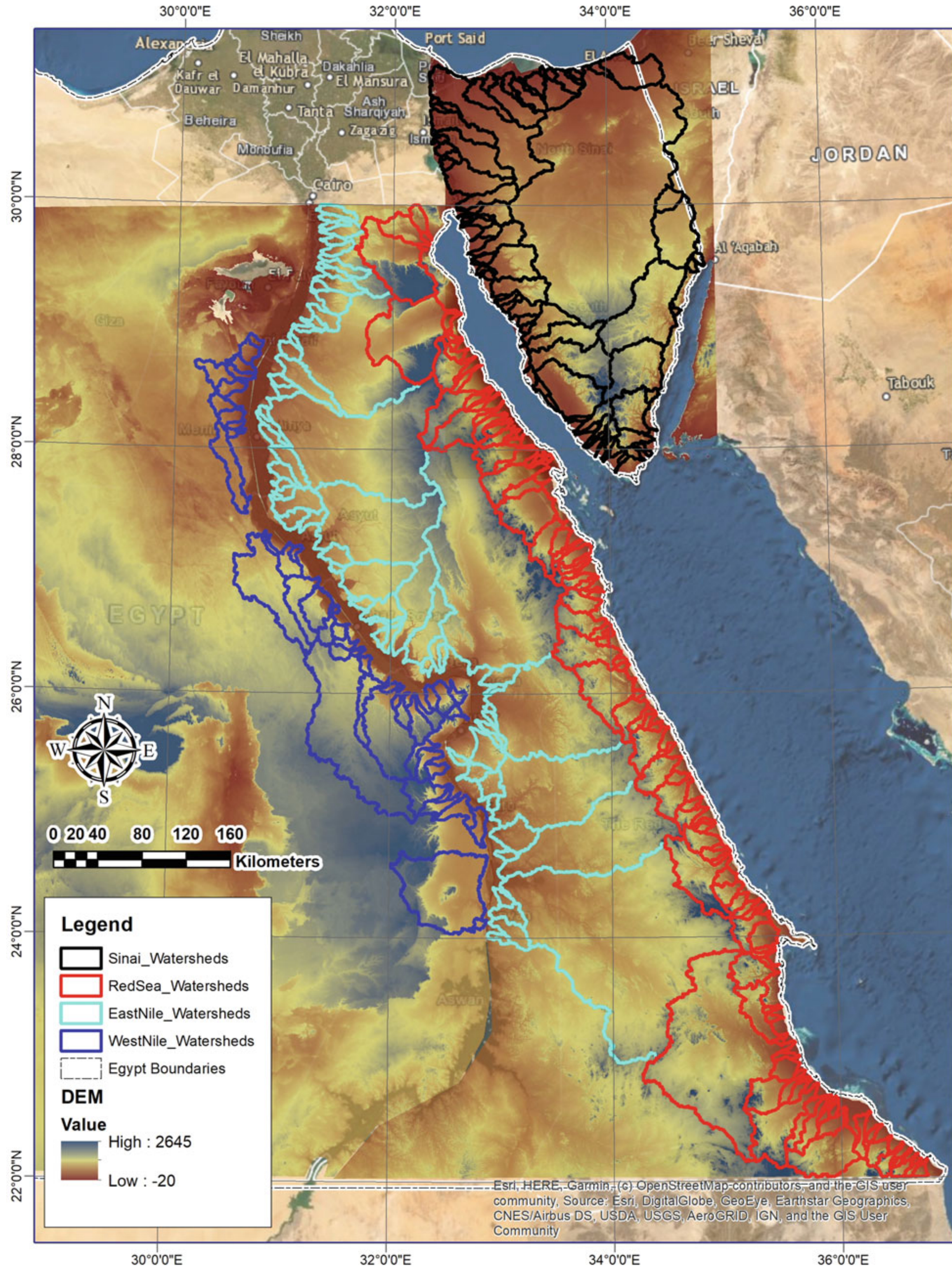


**Fig. 22** Digital Elevation Model (DEM) for the study area [SRTM 90 × 90]

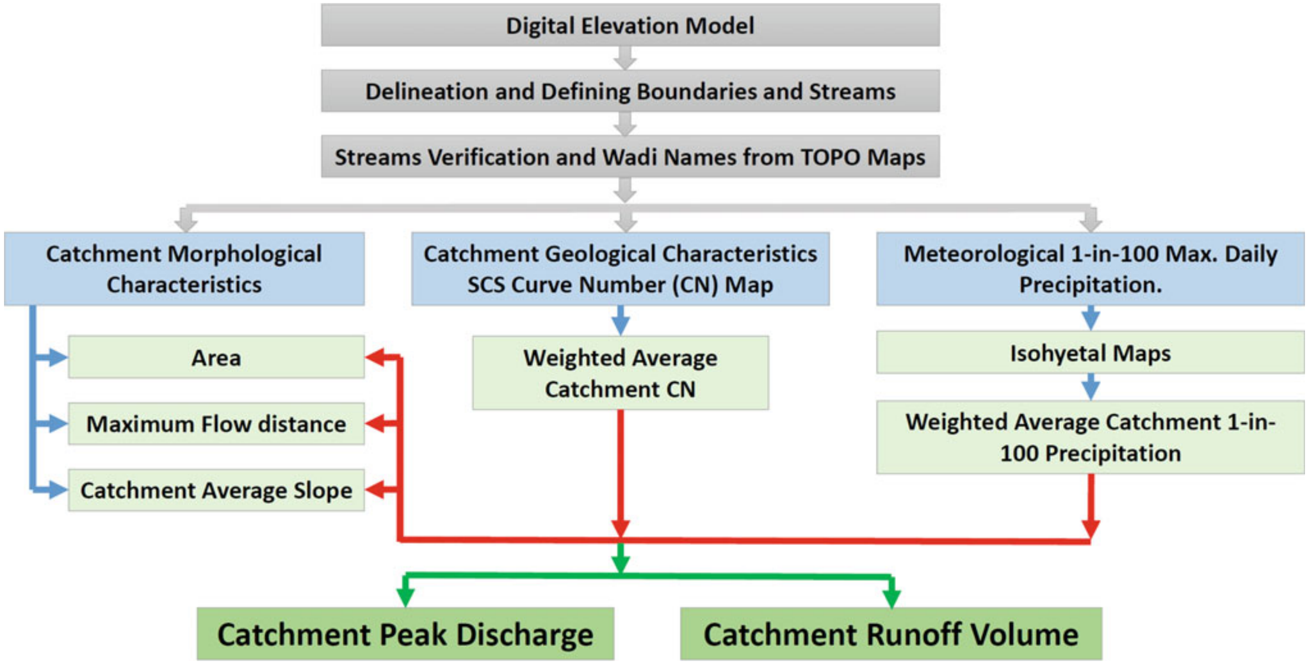


**Fig. 23** Flow chart for data processing procedure

**Table 2** Proposed risk categorization

| Risk category | Normalized risk factor range |
|---|---|
| Very high | 0.7–1.0 |
| High | 0.5–0.7 |
| Moderate | 0.3–0.5 |
| Low to moderate | 0.15–0.3 |
| Low | <0.15 |

$$T_p = 0.5D + T_L \quad (11)$$

where

$T_p$ Time to peak discharge (min)
$T_L$ Lag time = 0.6 × $T_c$ (min)
$D$ Rainfall duration in minutes corresponding to the time step of calculations where it is recommended not to exceed 0.133–0.2 $T_c$.

The catchment boundaries projected on SRTM 90 × 90 DEM raster and projected on topo maps, weighted average CN, and weighted average maximum daily precipitation for the 1-in-100 return period for each catchment area are shown in Fig. 26 through Fig. 29, respectively, for the Nile Region, Fig. 30 through Fig. 33 for the Red Sea region, and in Fig. 34 through Fig. 37 for Sinai Region. The summary of the catchment characteristics is given in Table 3 through Table 5 for the three studied regions.

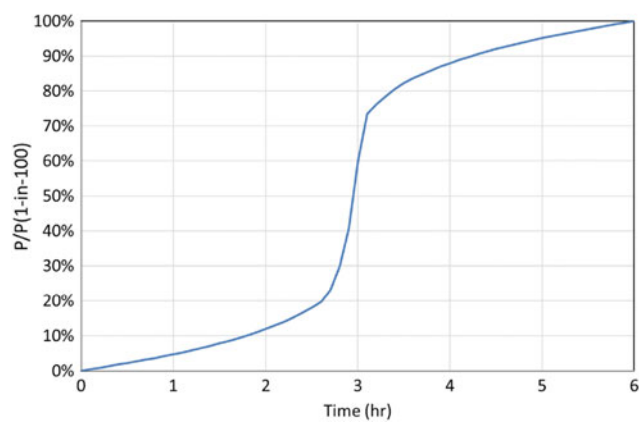


**Fig. 24** 6-h accumulated SCS type II storm distribution

## 7.5 Catchments Risk Assessment

Total runoff volume and peak discharge are characterized by their wide values range, a thoughtful assessment should be done before proceeding to the calculation of standardized risk factor. The box plot technique is utilized to eliminate the extreme values (Statistical outliers) that would lead to a misleading interpretation of the results. The concept of the box plot is shown in Fig. 38.

Following the limits provided in Table 6, the catchments with runoff volume and peak discharge above the maximum limit have been excluded from catchment categorization and considered as very high-risk catchments. Figure 39 through

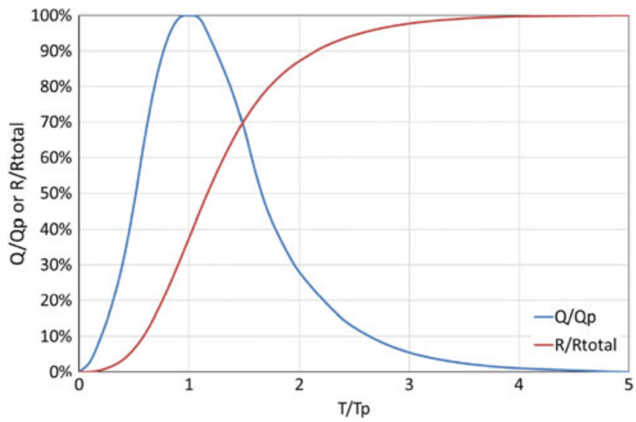


**Fig. 25** SCS dimensionless unit hydrograph and mass curve

Fig. 44 shows the results of risk catchments risk categorization for the studied regions based on Peak Flow Standardized Risk Factor (PFSRF) and Runoff Volume Standardized Risk Factor (RVSRF).

## 8 Decision Support System Work Plan

Classifying the drainage catchments located in Egypt based on a standardized risk assessment basis is the first step in supporting decision-makers to achieve the prioritization of the detailed risk assessment studies. The detailed risk assessment can be expanded into two further steps:

– The risk of wadies and/or reaches which can be provided with proper drainage structures to its final discharge points for 1-in-100 years return period design storm, can be reduced to a low-risk category after the implementation and the assurance of proper maintenance for flood mitigation measures. The storm harvesting in the form of artificial lakes, and dams can be selected as the first option in flood mitigation measures for the catchments associated with very high, and High Runoff Volume Risk Factor (RVSRF) to increase the rate of investment return from both flood mitigation and the reduction of freshwater stress.
– The wadies and/or reaches which cannot be provided with proper drainage to its final discharge points for 1-in-100 years return period design storm, two-dimensional modeling is mandatory for proper assessment of hazard, exposure, and vulnerability of the people and assets located in the flood plain. Figure 45 illustrates the workflow chart for risk assessment.

## 9 Determination of Flood Hazard Using Two-Dimensional Modeling

Ras-Gharib city was selected as a case study for flood intensity calculations. The delineated catchment for wadi Abou-Had using DEM files of resolution 30 × 30 m showed the original flow direction of the wadi toward its outfall far to the north of Ras-Gharib city, as shown in Figs. 46 and 47. The DEM-based delineation may be sufficient for a preliminary assessment for new lands, but for any human intervention, it is necessary to conduct a topographical survey for the area under study with proper expansion to capture the wadies sections.

Accordingly, it should be highlighted that the use of the DEM files is not sufficient to capture the manmade variations to the topology but in order to capture the real variation of the topology the actual survey of Ras-Gharib–El-Sheikh-Fadl road was added to the DEM file.

The 1-in-100 rainfall weighted average precipitation (53.53 mm) with 6 h SCS type II distribution, weighted average curve number (CN = 81.75), and updated DEM files were used to build a rainfall-runoff two-dimensional HEC-RAS model to track the streams attacking Ras-Gharib city. The model boundaries and flow depths are given in Fig. 48. Figures 49, 50, and 51 show a close view for the flow depth, velocity distribution, and the Flood Intensity (FI) within Ras-Gharib and surrounding areas, respectively.

$$\mathrm{FI} = V \times d \tag{12}$$

where

FI Flood intensity ($m^2/s$)
$V$ Flow Velocity (m/s)
$d$ Flow depth (m).

Due to the lack of field measurements during the flooding event, and in order to verify the results of the model; some flood plain photos were used and showed consistency with the model output as shown in Fig. 52. Achieving accurate assessment of risk requires a topographical survey to capture the buildings and streets which cannot be captured in the DEM file and will significantly impact the flow depth and velocity. Additionally, a land-use map has to be utilized to define the vulnerability to achieve a final risk map.

Additional updated two-dimensional HEC-RAS rainfall-runoff model has been conducted in order to assess the effectiveness of the newly constructed flood mitigation measures (the new culvert with attached two dikes). The results are given in Figs. 53, 54, and 55 show a significant reduction in flood intensity in Ras-Gharib city.

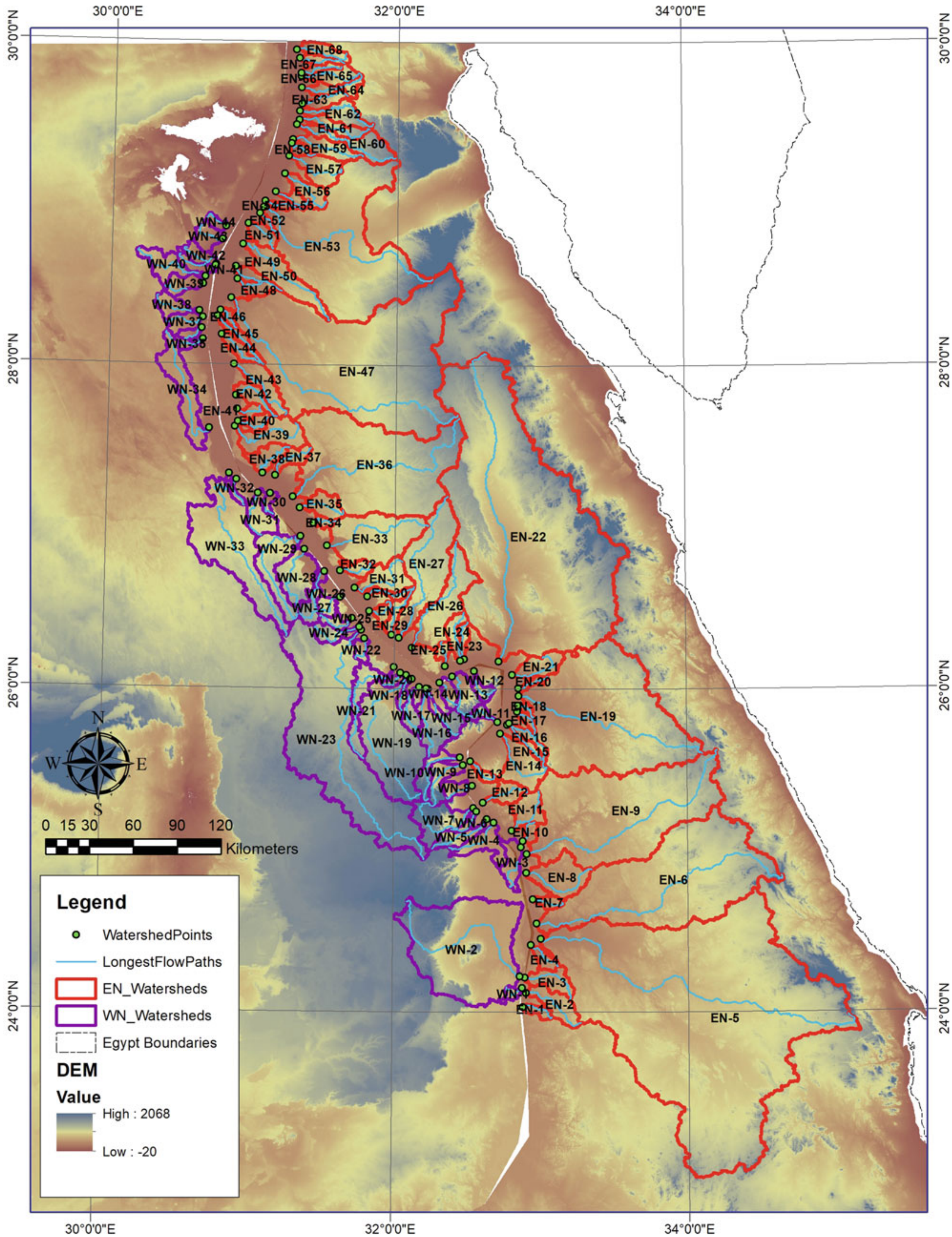


**Fig. 26** Projected Nile catchments on SRTM 90 × 90 DEM

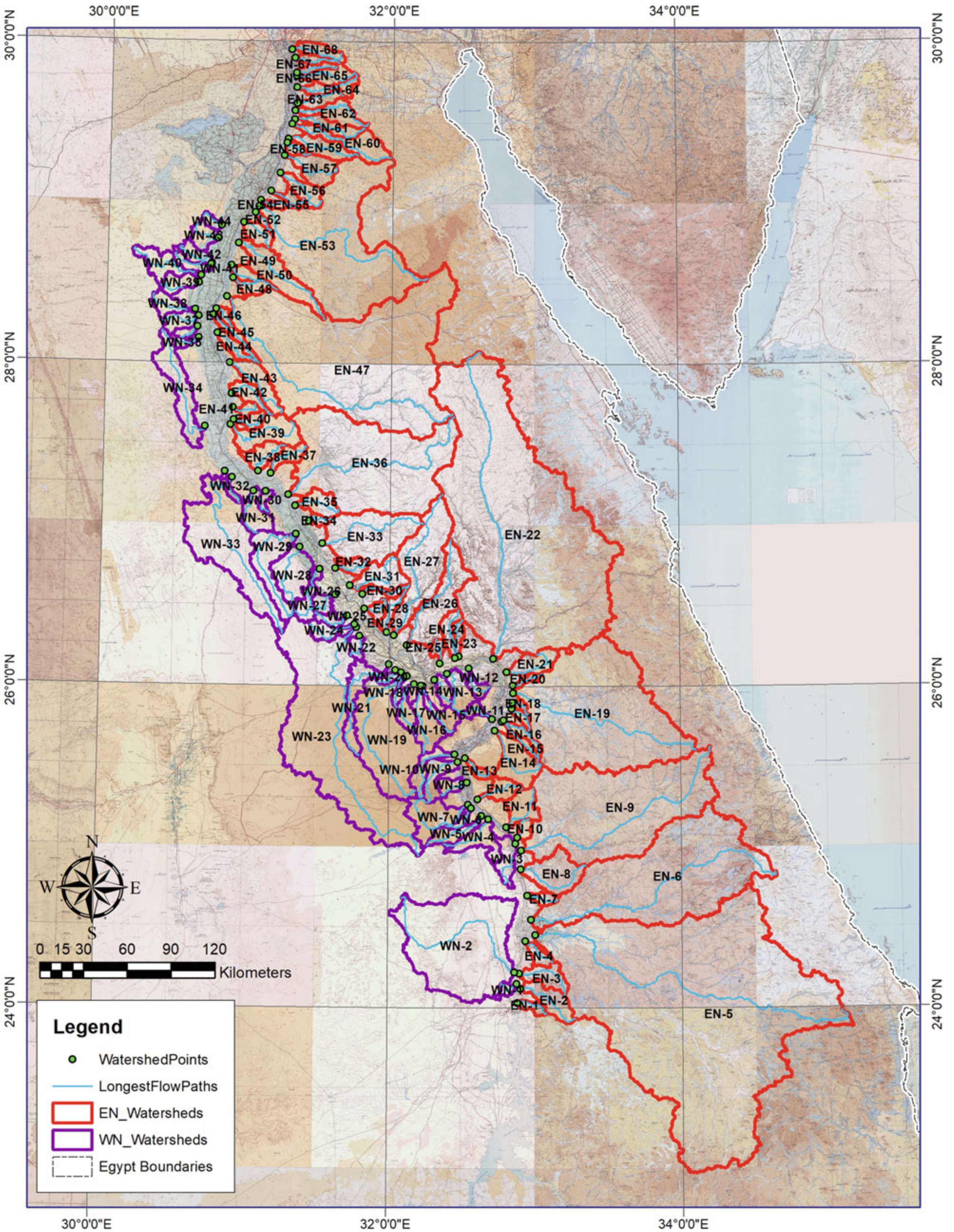


**Fig. 27** Projected Nile catchments on topo maps

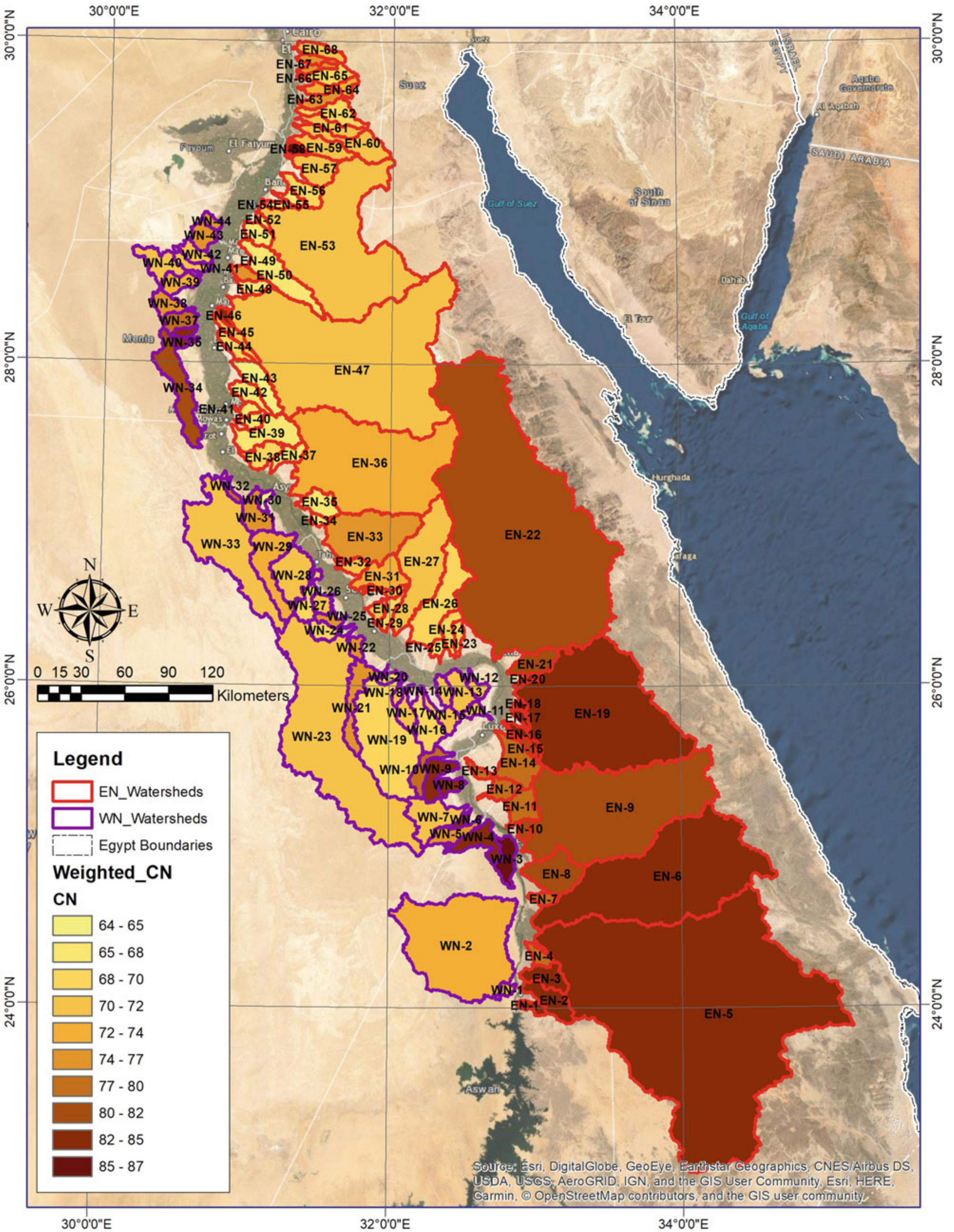


**Fig. 28** Nile catchments weighted average CN

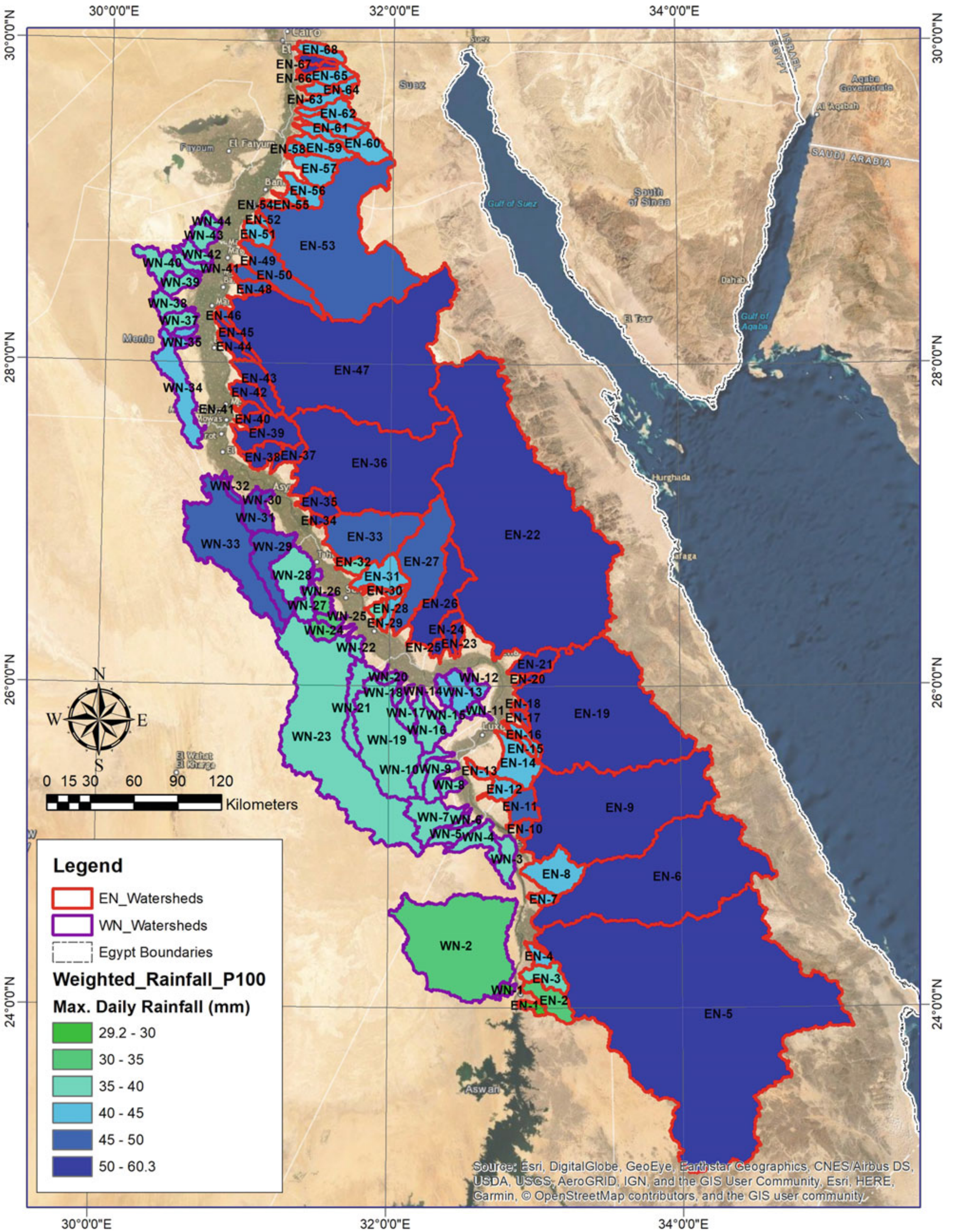


**Fig. 29** Nile catchments weighted average 1-in-100 maximum daily precipitation


**Fig. 30** Projected Red Sea catchments on SRTM 90 × 90 DEM

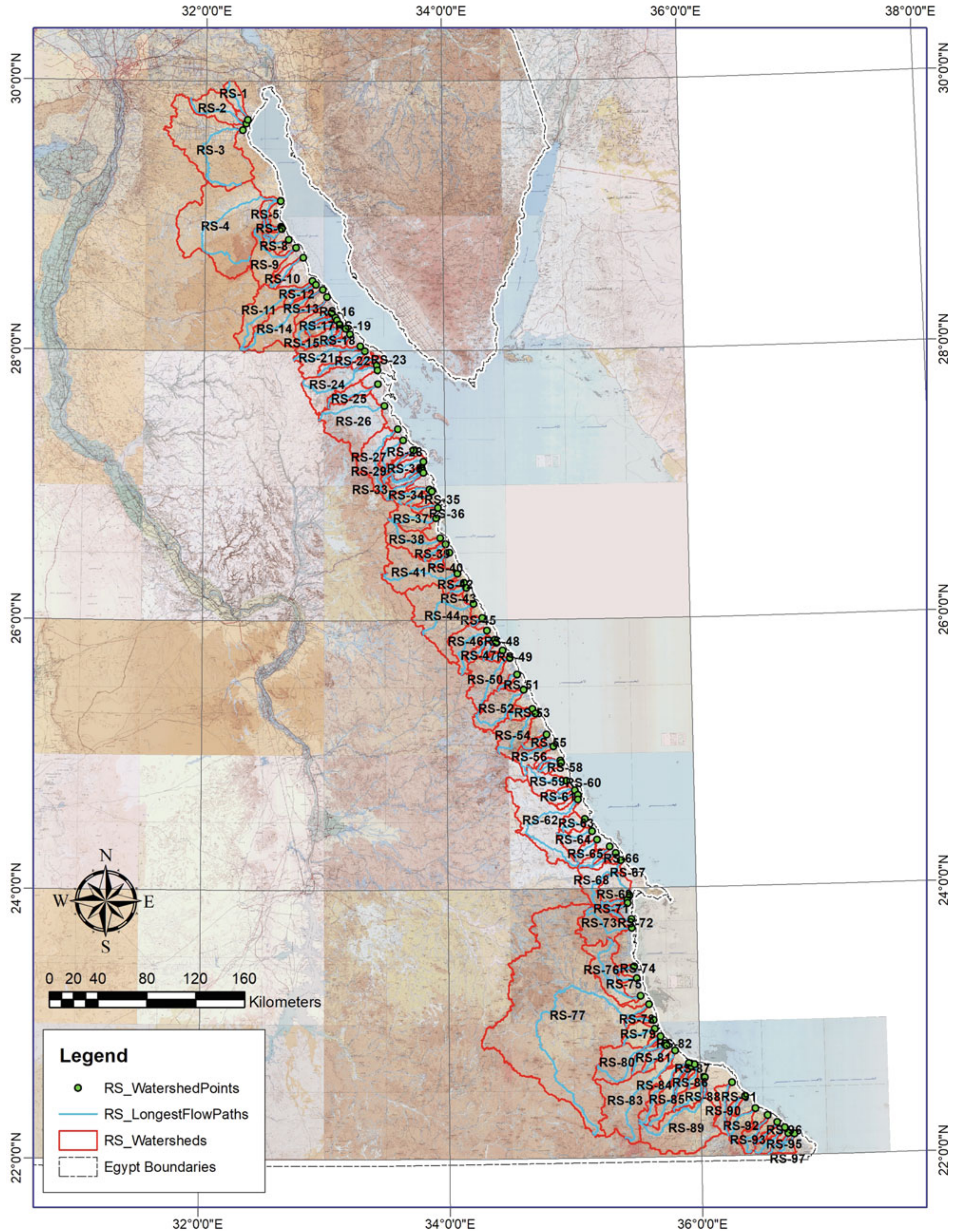


**Fig. 31** Projected Red Sea catchments on topo maps

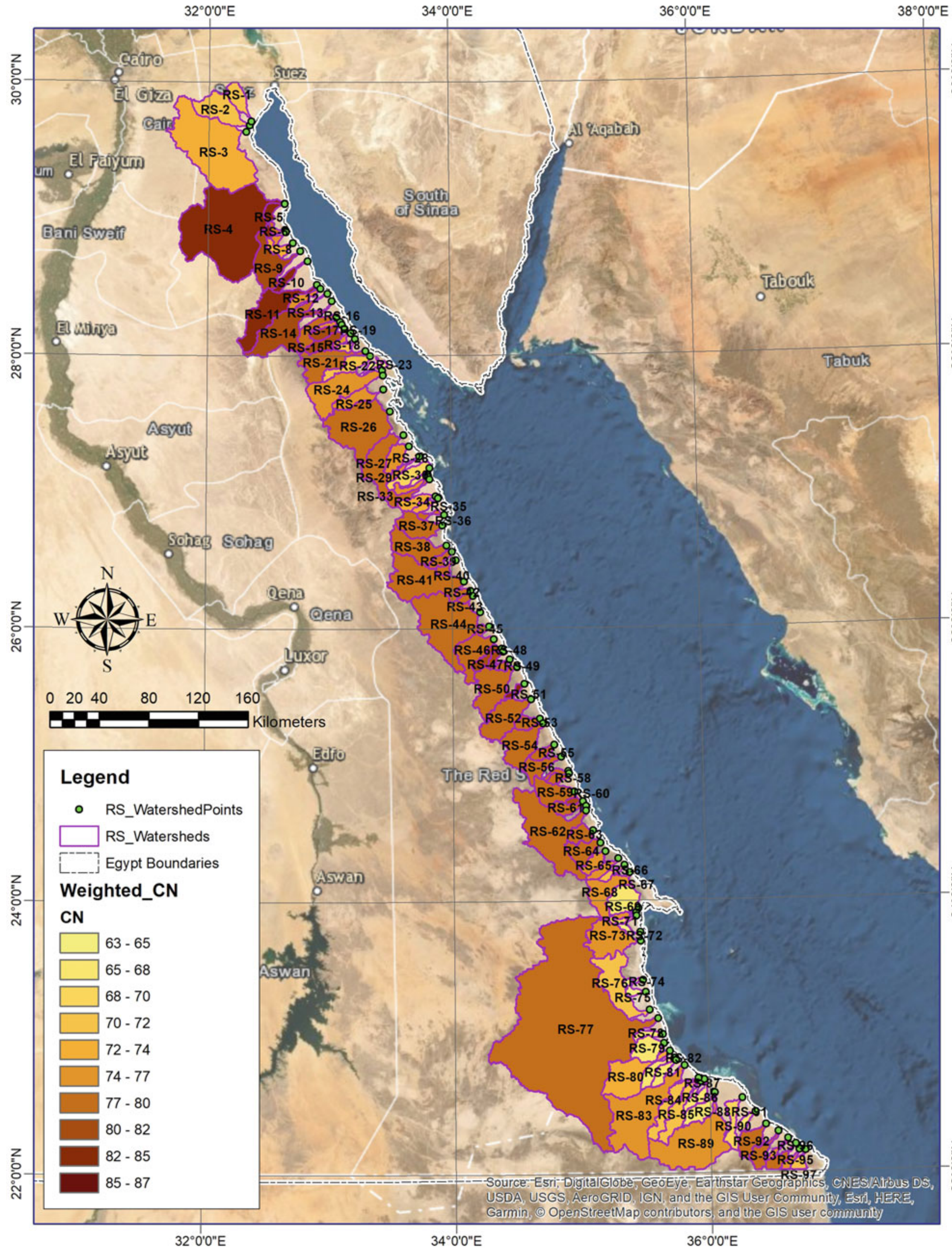


**Fig. 32** Red Sea catchments weighted average CN

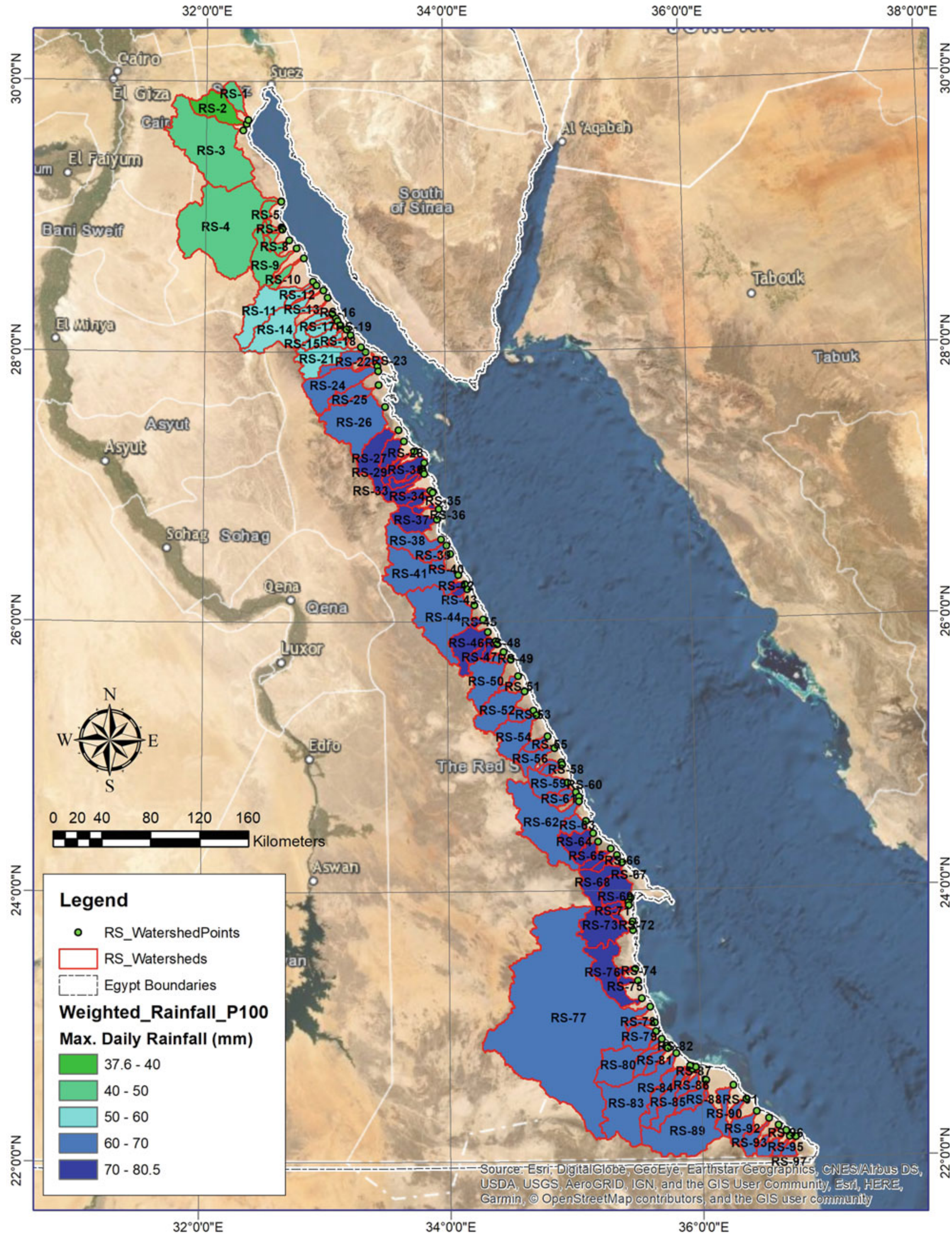


**Fig. 33** Red Sea catchments weighted average 1-in-100 maximum daily precipitation

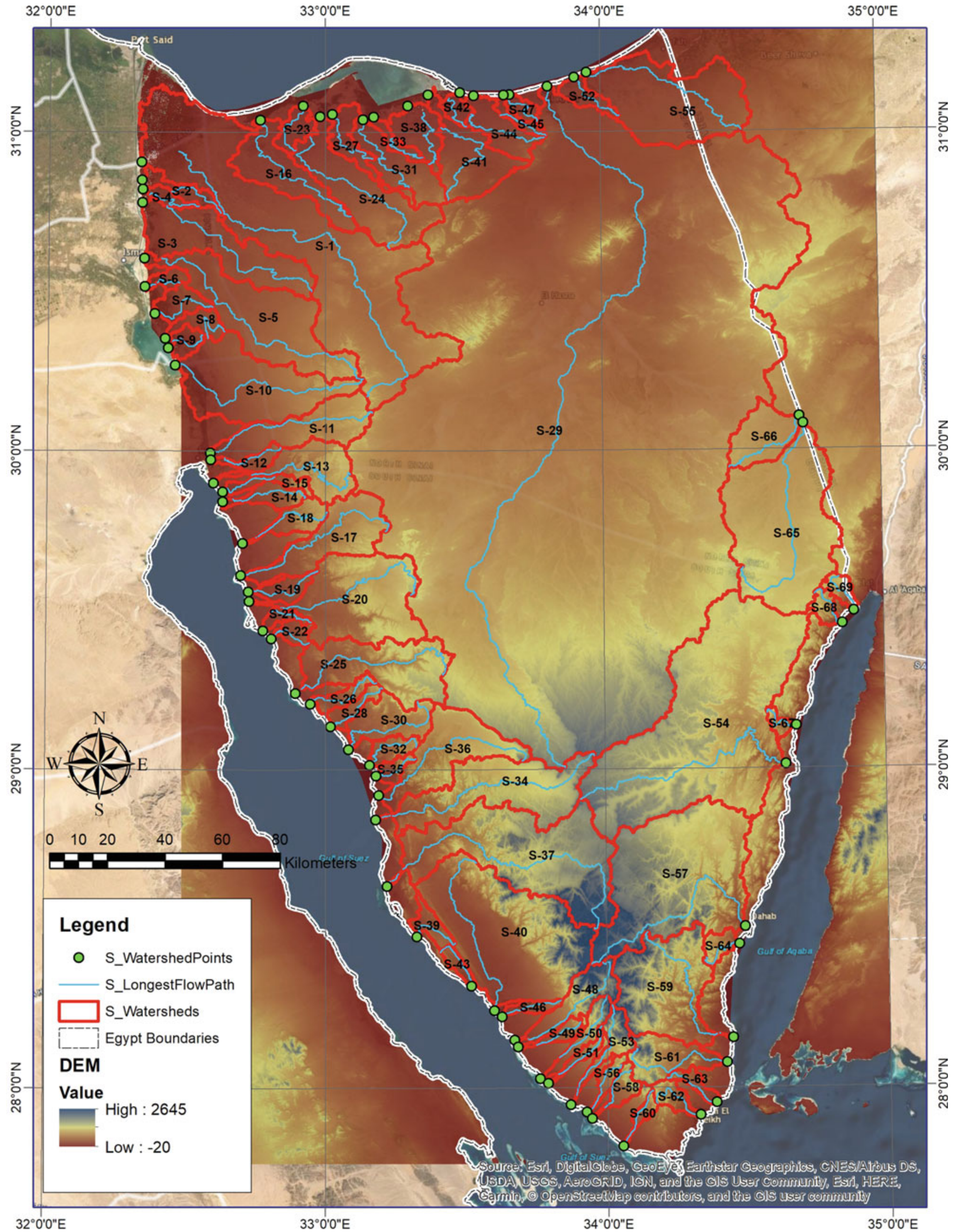


**Fig. 34** Projected Sinai catchments on SRTM 90 × 90 DEM

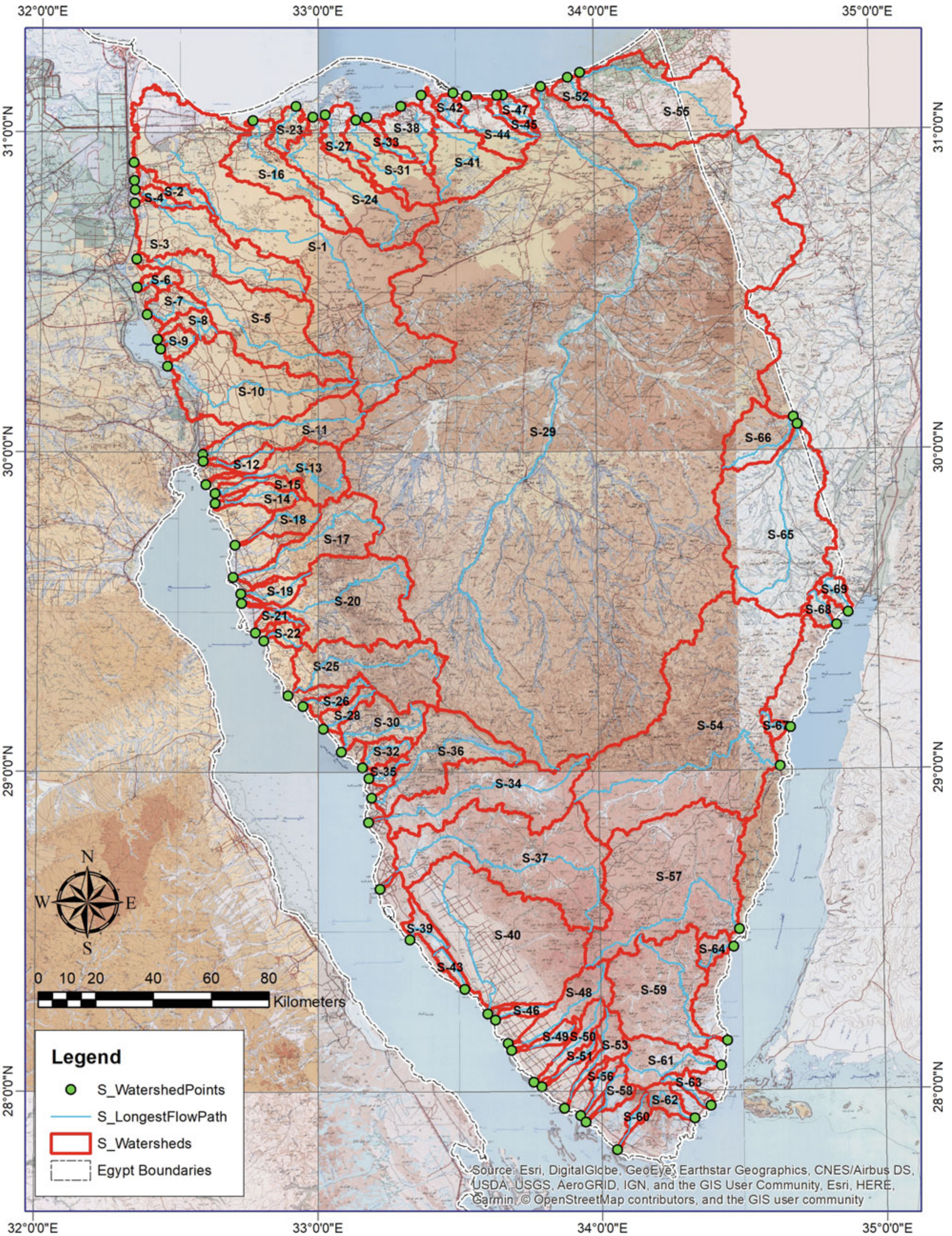


**Fig. 35** Projected Sinai catchments on topo maps

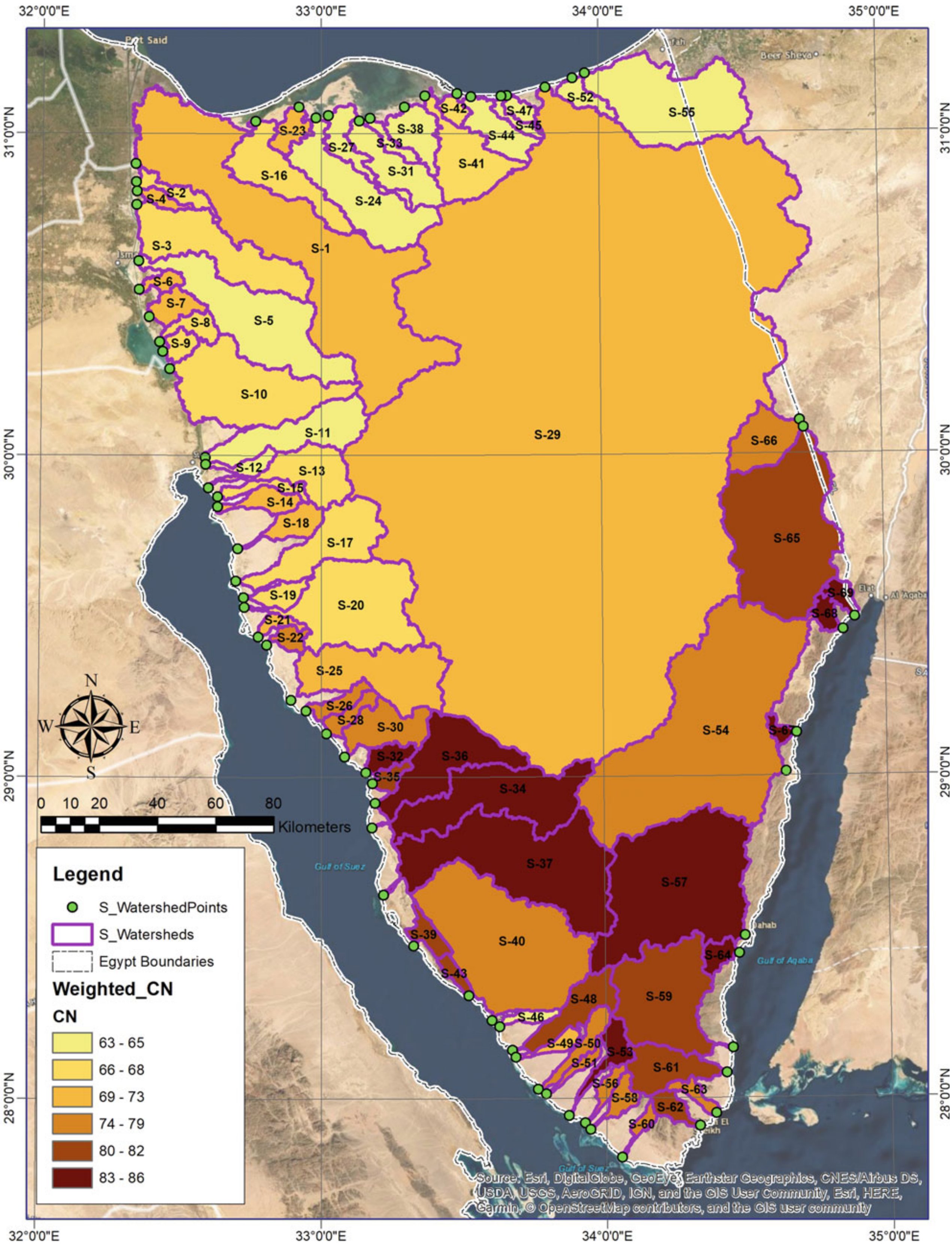


**Fig. 36** Sinai catchments weighted average CN

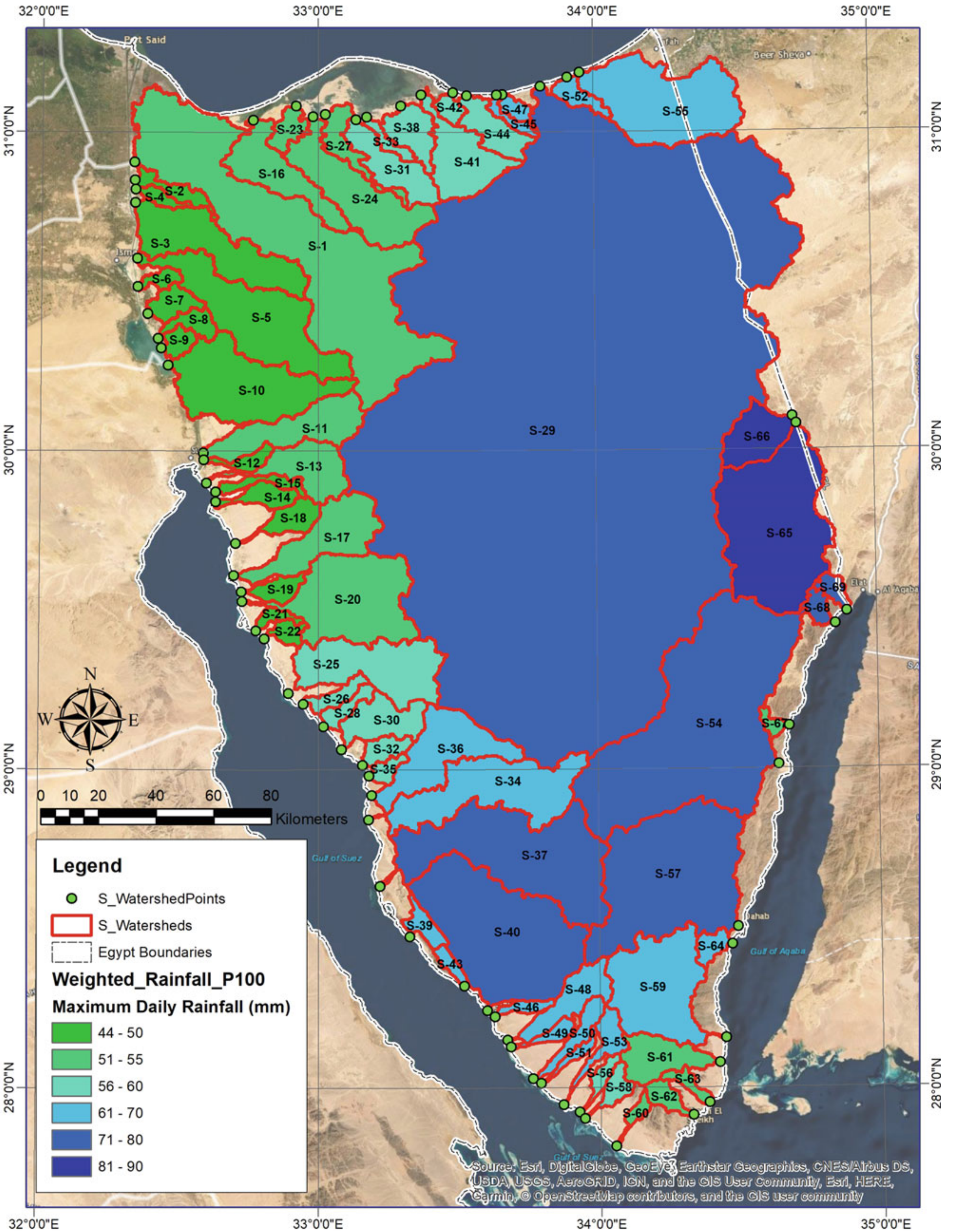


**Fig. 37** Sinai catchments weighted average 1-in-100 maximum daily precipitation

**Table 3** Nile river catchment characteristics

| Catchment No. | Wadi name | Area ($Km^2$) | CN | P100 (mm) | Runoff Vol (1000 $m^3$) |
|---|---|---|---|---|---|
| CA-EN-1 | Wadi Alakia | 120 | 84 | 29 | 669 |
| CA-EN-2 | Wadi Abou Aggag | 490 | 84 | 34 | 3,869 |
| CA-EN-3 | Wadi Abou Subaira | 394 | 84 | 37 | 4,061 |
| CA-EN-4 | Wadi Um Roukba | 163 | 79 | 41 | 1,284 |
| CA-EN-5 | Wadi Al Khurait | 21,076 | 85 | 53 | 456,716 |
| CA-EN-6 | Wadi Sheit | 7,156 | 82 | 52 | 126,771 |
| CA-EN-7 | Wadi AAied | 129 | 78 | 43 | 1,119 |
| CA-EN-8 | Wadi Al Serag | 822 | 81 | 45 | 9,224 |
| CA-EN-9 | Wadi Abbady | 6,749 | 82 | 52 | 116,494 |
| CA-EN-10 | Wadi Al Domi | 113 | 81 | 46 | 1,411 |
| CA-EN-11 | Wadi Hilal | 407 | 79 | 45 | 4,242 |
| CA-EN-12 | Wadi Al Shouki | 265 | 80 | 44 | 2,656 |
| CA-EN-13 | Wadi Abou Garawel | 102 | 80 | 42 | 935 |
| CA-EN-14 | Wadi Al Madamoud | 717 | 79 | 43 | 6,496 |
| CA-EN-15 | Wadi Banat Beri | 101 | 81 | 43 | 1,085 |
| CA-EN-16 | Wadi Gabal Al Nazi | 163 | 83 | 44 | 2,104 |
| CA-EN-17 | Wadi Hegaza | 84 | 84 | 46 | 1,357 |
| CA-EN-18 | Wadi Al Hagiat | 55 | 85 | 49 | 1,084 |
| CA-EN-19 | Wadi Al Qarn | 7,210 | 83 | 56 | 151,972 |
| CA-EN-20 | Wadi El Sheikh Eida | 81 | 83 | 56 | 1,734 |
| CA-EN-21 | Wadi El Seri | 404 | 81 | 58 | 8,234 |
| CA-EN-22 | Wadi Qena | 15,609 | 82 | 59 | 341,871 |
| CA-EN-23 | Wadi El Miat | 131 | 69 | 57 | 1,060 |
| CA-EN-24 | Wadi El Shikh Omar | 243 | 70 | 55 | 1,849 |
| CA-EN-25 | Wadi El Shikh Ali | 106 | 66 | 54 | 507 |
| CA-EN-26 | Wadi Abou Nafoukh | 1,238 | 70 | 51 | 7,730 |
| CA-EN-27 | Wadi Qasab | 1,940 | 72 | 48 | 12,396 |
| CA-EN-28 | Wadi Awlad Amar | 193 | 69 | 42 | 491 |
| CA-EN-29 | Wadi El Ahaywa | 134 | 71 | 39 | 386 |
| CA-EN-30 | Wadi Abou Gelbana | 117 | 72 | 40 | 397 |
| CA-EN-31 | Wadi Siflak | 564 | 72 | 40 | 2,082 |
| CA-EN-32 | Wadi Al Galawya | 173 | 71 | 38 | 466 |
| CA-EN-33 | Wadi Abou Shieh | 1,766 | 75 | 45 | 13,054 |
| CA-EN-34 | Wadi emo El Kebly | 78 | 67 | 53 | 395 |
| CA-EN-35 | Wadi eimo El Bahari | 359 | 67 | 54 | 1,926 |
| CA-EN-36 | Wadi El-Asiouty | 6,035 | 73 | 53 | 55,622 |
| CA-EN-37 | Wadi El Ibrahimi | 234 | 68 | 59 | 1,801 |
| CA-EN-38 | Wadi El Gabarawy | 322 | 69 | 60 | 2,897 |
| CA-EN-39 | Wadi Al Omrani | 739 | 67 | 58 | 5,133 |
| CA-EN-40 | Wadi Abu Hasah | 149 | 65 | 57 | 815 |
| CA-EN-41 | Wadi Alrashawy | 110 | 65 | 56 | 574 |
| CA-EN-42 | Wadi El Maree | 271 | 66 | 55 | 1,323 |
| CA-EN-43 | Wadi Al Mushakkak | 500 | 64 | 54 | 1,932 |
| CA-EN-44 | Wadi Al Tahnawy | 209 | 69 | 51 | 1,185 |

(continued)

**Table 3** (continued)

| Catchment No. | Wadi name | Area ($Km^2$) | CN | P100 (mm) | Runoff Vol (1000 $m^3$) |
|---|---|---|---|---|---|
| CA-EN-45 | Wadi Garf El Deir | 204 | 70 | 51 | 1,266 |
| CA-EN-46 | Wadi Sarirya | 80 | 82 | 49 | 1,286 |
| CA-EN-47 | Wadi Al tourka | 10,607 | 71 | 51 | 71,216 |
| CA-EN-48 | Wadi El Mohashm | 199 | 65 | 47 | 532 |
| CA-EN-49 | Wadi Sharouna | 152 | 75 | 47 | 1,153 |
| CA-EN-50 | Wadi El Sheikh | 908 | 65 | 47 | 2,337 |
| CA-EN-51 | Wadi El Fakira | 244 | 67 | 45 | 643 |
| CA-EN-52 | Wadi Ghayada | 64 | 65 | 44 | 122 |
| CA-EN-53 | Wadi Sanour | 6,241 | 70 | 46 | 27,987 |
| CA-EN-54 | Wadi Rood Ghorab | 97 | 66 | 43 | 199 |
| CA-EN-55 | Wadi Bayad | 121 | 66 | 43 | 258 |
| CA-EN-56 | Wadi Al Shoyab | 327 | 69 | 43 | 1,066 |
| CA-EN-57 | Wadi Ramlya | 498 | 70 | 43 | 1,710 |
| CA-EN-58 | Wadi Gabal Tarbool | 107 | 87 | 43 | 1,847 |
| CA-EN-59 | Wadi El Atfihi | 425 | 72 | 42 | 1,720 |
| CA-EN-60 | Wadi El Rashah | 629 | 71 | 42 | 2,239 |
| CA-EN-61 | Wadi El Neomia | 303 | 71 | 42 | 1,160 |
| CA-EN-62 | Wadi El Wadag | 430 | 69 | 42 | 1,215 |
| CA-EN-63 | Wadi Um Ramath | 210 | 77 | 45 | 1,732 |
| CA-EN-64 | Wadi Al Hira | 267 | 72 | 44 | 1,277 |
| CA-EN-65 | Wadi Um Hassan | 313 | 69 | 45 | 1,183 |
| CA-EN-66 | Wadi El Mahalawya | 115 | 77 | 51 | 1,286 |
| CA-EN-67 | Wadi Houf | 127 | 75 | 51 | 1,253 |
| CA-EN-68 | Wadi Degla | 252 | 71 | 43 | 961 |
| CA-WN-1 | Wadi Al-Kotb | 89 | 71 | 29 | 51 |
| CA-WN-2 | Wadi Al-Kobania | 4,595 | 71 | 39 | 12,363 |
| CA-WN-3 | Wadi-Al-Kara | 337 | 86 | 44 | 5,860 |
| CA-WN-4 | Wadi-Elhami | 461 | 82 | 45 | 5,718 |
| CA-WN-5 | Wadi-Koum-Meir | 290 | 72 | 45 | 1,558 |
| CA-WN-6 | Wadi-Abou-Aad | 72 | 80 | 45 | 812 |
| CA-WN-7 | Wadi-Esna | 722 | 69 | 45 | 2,781 |
| CA-WN-8 | Wadi-Al-Rokham | 169 | 85 | 44 | 2,584 |
| CA-WN-9 | Wadi-El-Mahameed | 369 | 83 | 45 | 5,168 |
| CA-WN-10 | – | 304 | 75 | 46 | 2,249 |
| CA-WN-11 | – | 110 | 68 | 46 | 366 |
| CA-WN-12 | – | 138 | 70 | 54 | 1,055 |
| CA-WN-13 | – | 372 | 69 | 51 | 2,093 |
| CA-WN-14 | – | 181 | 68 | 51 | 902 |
| CA-WN-15 | – | 268 | 68 | 47 | 972 |
| CA-WN-16 | – | 521 | 67 | 47 | 1,795 |
| CA-WN-17 | – | 247 | 70 | 48 | 1,200 |
| CA-WN-18 | – | 92 | 69 | 48 | 427 |
| CA-WN-19 | – | 2,497 | 67 | 47 | 8,499 |

(continued)

**Table 3** (continued)

| Catchment No. | Wadi name | Area ($Km^2$) | CN | P100 (mm) | Runoff Vol (1000 $m^3$) |
|---|---|---|---|---|---|
| CA-WN-20 | – | 80 | 66 | 48 | 243 |
| CA-WN-21 | Wadi-Samhoud | 586 | 72 | 46 | 3,408 |
| CA-WN-22 | – | 128 | 73 | 42 | 587 |
| CA-WN-23 | – | 6,341 | 68 | 46 | 22,760 |
| CA-WN-24 | Wadi El-Yateem | 221 | 67 | 40 | 353 |
| CA-WN-25 | Wadi-Tag-El-Deir | 137 | 72 | 38 | 402 |
| CA-WN-26 | Wadi-Abou-Retag | 167 | 70 | 37 | 331 |
| CA-WN-27 | Wadi-Juhaina | 302 | 66 | 41 | 460 |
| CA-WN-28 | Wadi-Darb-El-Ghanayem | 743 | 68 | 48 | 3,106 |
| CA-WN-29 | Wadi-Serga | 913 | 70 | 56 | 7,705 |
| CA-WN-30 | – | 89 | 64 | 65 | 651 |
| CA-WN-31 | – | 405 | 73 | 66 | 6,328 |
| CA-WN-32 | – | 71 | 77 | 65 | 1,355 |
| CA-WN-33 | – | 2,696 | 70 | 60 | 26,814 |
| CA-WN-34 | – | 947 | 78 | 54 | 12,901 |
| CA-WN-35 | – | 92 | 81 | 51 | 1,377 |
| CA-WN-36 | – | 88 | 82 | 50 | 1,387 |
| CA-WN-37 | – | 262 | 77 | 49 | 2,781 |
| CA-WN-38 | – | 268 | 73 | 49 | 1,976 |
| CA-WN-39 | – | 268 | 71 | 47 | 1,426 |
| CA-WN-40 | – | 486 | 68 | 46 | 1,658 |
| CA-WN-41 | – | 166 | 69 | 46 | 700 |
| CA-WN-42 | – | 212 | 69 | 46 | 832 |
| CA-WN-43 | – | 262 | 72 | 45 | 1,366 |
| CA-WN-44 | – | 96 | 73 | 44 | 529 |

**Table 4** Red Sea catchment characteristics

| Catchment no. | Wadi name | Area ($Km^2$) | CN | P100 (mm) | Runoff Vol (1000 $m^3$) |
|---|---|---|---|---|---|
| CA-RS-1 | Wadi Hagoul | 274 | 72 | 43 | 1,225 |
| CA-RS-2 | Wadi Bedaa | 687 | 71 | 38 | 1,703 |
| CA-RS-3 | Wadi Ghoweba | 2,882 | 73 | 40 | 11,505 |
| CA-RS-4 | Wadi Araba | 3,910 | 84 | 45 | 57,134 |
| CA-RS-5 | Wadi Gabal Thalmat | 183 | 84 | 46 | 2,773 |
| CA-RS-6 | Wadi El Garph | 53 | 80 | 46 | 597 |
| CA-RS-7 | Wadi Al Beir | 51 | 77 | 47 | 470 |
| CA-RS-8 | Wadi Abou Khalifi | 150 | 74 | 48 | 1,102 |
| CA-RS-9 | Wadi Al Dahl | 741 | 82 | 48 | 10,828 |
| CA-RS-10 | Wadi North Wadi Houshya | 148 | 84 | 50 | 2,742 |
| CA-RS-11 | Wadi Hawashia North | 1,020 | 82 | 51 | 17,604 |
| CA-RS-12 | Wadi Hawashia South | 158 | 76 | 52 | 1,750 |
| CA-RS-13 | Wadi West Bakr Wells | 99 | 79 | 53 | 1,479 |

(continued)

**Table 4** (continued)

| Catchment no. | Wadi name | Area (Km$^2$) | CN | P100 (mm) | Runoff Vol (1000 m$^3$) |
|---|---|---|---|---|---|
| CA-RS-14 | Wadi Abou Had | 1,048 | 82 | 54 | 18,862 |
| CA-RS-15 | Wadi EL Darb | 279 | 79 | 55 | 4,470 |
| CA-RS-16 | Wadi Hareem | 66 | 77 | 56 | 931 |
| CA-RS-17 | Wadi Um Yousr | 170 | 81 | 56 | 3,161 |
| CA-RS-18 | Wadi Ghareb | 247 | 80 | 57 | 4,602 |
| CA-RS-19 | Wadi Kharm El Oyoun | 62 | 75 | 59 | 846 |
| CA-RS-20 | Wadi Garph | 80 | 72 | 60 | 911 |
| CA-RS-21 | Wadi North Wadi Dara | 723 | 80 | 59 | 14,026 |
| CA-RS-22 | Wadi Dara | 313 | 71 | 62 | 3,738 |
| CA-RS-23 | Wadi Noth Wadi Dob | 92 | 64 | 65 | 683 |
| CA-RS-24 | Wadi Dob | 1,045 | 77 | 63 | 18,635 |
| CA-RS-25 | Wadi Abou Had (hurgada) | 325 | 74 | 66 | 5,687 |
| CA-RS-26 | Wadi Malaha | 1,659 | 78 | 70 | 40,612 |
| CA-RS-27 | Wadi Biali | 735 | 79 | 74 | 21,159 |
| CA-RS-28 | Wadi Kharaza | 282 | 74 | 78 | 7,014 |
| CA-RS-29 | Wadi Abou Malaka | 104 | 74 | 78 | 2,549 |
| CA-RS-30 | Wadi Falek Al Sahl | 318 | 69 | 79 | 5,863 |
| CA-RS-31 | Wadi Um Dalfa | 65 | 65 | 79 | 922 |
| CA-RS-32 | Wadi Abou Eid | 127 | 74 | 77 | 3,048 |
| CA-RS-33 | Wadi Um Gudari | 196 | 78 | 74 | 5,426 |
| CA-RS-34 | Wadi Um Kbash | 213 | 74 | 74 | 4,559 |
| CA-RS-35 | Wadi El Mamal | 100 | 72 | 74 | 1,967 |
| CA-RS-36 | Wadi Al Mowasala | 70 | 78 | 72 | 1,831 |
| CA-RS-37 | Wadi Al Baroud | 506 | 80 | 70 | 13,449 |
| CA-RS-38 | Wadi Safaga | 716 | 79 | 67 | 17,069 |
| CA-RS-39 | Wadi Gasous | 137 | 80 | 69 | 3,586 |
| CA-RS-40 | Wadi Abou Shoukaili | 100 | 78 | 70 | 2,468 |
| CA-RS-41 | Wadi Al Kareeh | 1,390 | 78 | 67 | 31,089 |
| CA-RS-42 | Wadi Abou Oumra | 62 | 77 | 73 | 1,600 |
| CA-RS-43 | Wadi El Hadadeen | 60 | 78 | 74 | 1,635 |
| CA-RS-44 | Wadi El Nakheel | 1,906 | 78 | 70 | 47,098 |
| CA-RS-45 | Wadi El Zarib | 55 | 78 | 75 | 1,537 |
| CA-RS-46 | Wadi Esl | 631 | 79 | 71 | 16,245 |
| CA-RS-47 | Wadi Sharm El Bahari | 176 | 80 | 71 | 4,901 |
| CA-RS-48 | Wadi Sharm El Kebly | 92 | 80 | 71 | 2,621 |
| CA-RS-49 | Wadi Wazar | 67 | 79 | 70 | 1,688 |
| CA-RS-50 | Wadi Um Lasifa | 841 | 80 | 66 | 20,330 |
| CA-RS-51 | Wadi Um Grifi | 71 | 84 | 66 | 2,186 |
| CA-RS-52 | Wadi Mubarak | 785 | 79 | 63 | 16,187 |
| CA-RS-53 | Wadi Abou Dabbab | 165 | 77 | 63 | 3,082 |
| CA-RS-54 | Wadi El Nabe | 742 | 78 | 61 | 13,631 |
| CA-RS-55 | Wadi Egla | 134 | 79 | 62 | 2,736 |

(continued)

**Table 4** (continued)

| Catchment no. | Wadi name | Area (Km$^2$) | CN | P100 (mm) | Runoff Vol (1000 m$^3$) |
|---|---|---|---|---|---|
| CA-RS-56 | Wadi Um Harika | 315 | 78 | 62 | 5,856 |
| CA-RS-57 | Wadi Um Tandia | 66 | 79 | 63 | 1,341 |
| CA-RS-58 | Wadi El ambaout | 95 | 78 | 63 | 1,832 |
| CA-RS-59 | Wadi Ghadir | 486 | 78 | 63 | 9,782 |
| CA-RS-60 | Wadi Sharm Al Foukairy | 56 | 81 | 66 | 1,396 |
| CA-RS-61 | Wadi Arear | 195 | 77 | 65 | 4,019 |
| CA-RS-62 | Wadi Al Gemal | 1,951 | 79 | 65 | 44,347 |
| CA-RS-63 | Wadi Um Al Abs | 236 | 78 | 70 | 5,596 |
| CA-RS-64 | Wadi Abou Ghousoun | 368 | 78 | 72 | 9,177 |
| CA-RS-65 | Wadi Al Renga | 210 | 77 | 75 | 5,444 |
| CA-RS-66 | Wadi El Rada | 157 | 75 | 77 | 3,799 |
| CA-RS-67 | Wadi Al Khasheer | 88 | 71 | 78 | 1,794 |
| CA-RS-68 | Wadi Lahmi | 592 | 74 | 78 | 14,594 |
| CA-RS-69 | Wadi Naaeet | 484 | 68 | 81 | 8,662 |
| CA-RS-70 | Wadi Um Selem | 62 | 75 | 80 | 1,673 |
| CA-RS-71 | Wadi Kalalat | 79 | 69 | 80 | 1,503 |
| CA-RS-72 | Wadi Kntroub | 62 | 64 | 80 | 826 |
| CA-RS-73 | Wadi Khada | 836 | 75 | 77 | 21,352 |
| CA-RS-74 | Wadi Marafai | 63 | 65 | 75 | 742 |
| CA-RS-75 | Wadi Klibtab | 77 | 63 | 74 | 773 |
| CA-RS-76 | Wadi El Rahba | 950 | 71 | 73 | 16,804 |
| CA-RS-77 | Wadi Houdein | 11,577 | 80 | 64 | 265,779 |
| CA-RS-78 | Wadi Al Wadah | 111 | 66 | 69 | 1,194 |
| CA-RS-79 | Wadi Safira | 391 | 68 | 68 | 4,587 |
| CA-RS-80 | Wadi Sab | 906 | 73 | 65 | 13,971 |
| CA-RS-81 | Wadi Amrawy El Bahary | 225 | 68 | 66 | 2,447 |
| CA-RS-82 | Wadi Amrawy El Kebly | 180 | 68 | 66 | 1,973 |
| CA-RS-83 | Wadi Eib | 1,969 | 75 | 63 | 32,262 |
| CA-RS-84 | Wadi Maysa-2 | 465 | 71 | 64 | 6,014 |
| CA-RS-85 | Wad Andri | 479 | 71 | 64 | 5,765 |
| CA-RS-86 | Wadi Maysa-1 | 118 | 68 | 65 | 1,216 |
| CA-RS-87 | Wadi Ramram | 92 | 68 | 65 | 965 |
| CA-RS-88 | Wadi Halal Rahandeeb | 318 | 68 | 64 | 3,189 |
| CA-RS-89 | Wadi Deib | 1,925 | 75 | 62 | 30,737 |
| CA-RS-90 | Wadi Daeit | 301 | 70 | 63 | 3,372 |
| CA-RS-91 | Wadi Bashoya | 95 | 68 | 64 | 940 |
| CA-RS-92 | Wadi Yowayder | 352 | 78 | 63 | 6,768 |
| CA-RS-93 | Wadi Sarmatai | 243 | 78 | 62 | 4,723 |
| CA-RS-94 | Wadi Merakwan | 72 | 76 | 62 | 1,191 |
| CA-RS-95 | Wadi Shallal | 180 | 77 | 62 | 3,263 |
| CA-RS-96 | Wadi Aklahok | 82 | 76 | 62 | 1,323 |
| CA-RS-97 | Wadi Ay Kawan | 111 | 70 | 62 | 1,231 |

**Table 5** Sinai catchment characteristics

| Catchment no. | Wadi name | Area ($Km^2$) | CN | P100 (mm) | Runoff Vol (1000 $m^3$) |
|---|---|---|---|---|---|
| CA-S-1 | Wadi-Abou Amer | 3,446 | 68 | 51 | 18,224 |
| CA-S-2 | Wadi-El Kantara Sharq-1 | 137 | 67 | 46 | 401 |
| CA-S-3 | Wadi-Mardoum | 870 | 65 | 47 | 2,359 |
| CA-S-4 | Wadi-El Kantara Sharq-2 | 68 | 68 | 45 | 225 |
| CA-S-5 | Wadi-Elwa | 1,199 | 65 | 49 | 3,282 |
| CA-S-6 | Wadi-Talia | 71 | 73 | 44 | 384 |
| CA-S-7 | Wadi-Khoubaita | 156 | 71 | 45 | 705 |
| CA-S-8 | Wadi-El-Habashi-North | 122 | 66 | 46 | 321 |
| CA-S-9 | Wadi-El-Habashi-South | 93 | 68 | 46 | 298 |
| CA-S-10 | Wadi-El Gadi | 1,120 | 66 | 49 | 3,584 |
| CA-S-11 | Wadi-El Mor-1 | 607 | 64 | 51 | 1,805 |
| CA-S-12 | Wadi-El Mor-2 | 93 | 64 | 49 | 216 |
| CA-S-13 | Wadi-El Raha | 442 | 68 | 51 | 2,099 |
| CA-S-14 | Wadi-El Rabina | 150 | 68 | 49 | 630 |
| CA-S-15 | Wadi-Um Asagil | 104 | 67 | 49 | 381 |
| CA-S-16 | Wadi-Um Okba | 555 | 67 | 50 | 2,264 |
| CA-S-17 | Wadi-Sedr | 631 | 67 | 51 | 2,664 |
| CA-S-18 | Wadi-Lhata | 178 | 71 | 49 | 1,094 |
| CA-S-19 | Wadi-Roud El Raha | 129 | 65 | 47 | 341 |
| CA-S-20 | Wadi-Werdan | 1,148 | 68 | 54 | 6,468 |
| CA-S-21 | Wadi-Abou Hagar North | 63 | 72 | 48 | 382 |
| CA-S-22 | Wadi-Abou Hagar South | 81 | 78 | 49 | 931 |
| CA-S-23 | Wadi-El Kantara | 134 | 71 | 51 | 897 |
| CA-S-24 | Wadi-El Beada | 838 | 64 | 54 | 3,187 |
| CA-S-25 | Wadi Gharandal | 861 | 69 | 57 | 7,002 |
| CA-S-26 | Wadi-Waset | 113 | 76 | 56 | 1,499 |
| CA-S-27 | Wadi-El Sadat | 221 | 65 | 54 | 915 |
| CA-S-28 | Wadi-Tal | 108 | 74 | 57 | 1,248 |
| CA-S-29 | Wadi-El Arish | 23,669 | 70 | 73 | 386,253 |
| CA-S-30 | Wadi-Taiba | 357 | 77 | 58 | 5,788 |
| CA-S-31 | Wadi-El Abd | 394 | 64 | 55 | 1,616 |
| CA-S-32 | Wadi-Nakhl | 121 | 84 | 58 | 2,871 |
| CA-S-33 | Wadi-Musafak | 75 | 64 | 55 | 298 |
| CA-S-34 | Wadi-Sedri | 1,074 | 84 | 68 | 33,789 |
| CA-S-35 | Wadi-Defri | 74 | 81 | 58 | 1,541 |
| CA-S-36 | Wadi-Bobo | 718 | 83 | 62 | 18,613 |
| CA-S-37 | Wadi-Firan | 1,780 | 83 | 73 | 62,523 |
| CA-S-38 | Wad-El Artah | 262 | 63 | 56 | 1,092 |
| CA-S-39 | Wadi-Araba North | 115 | 81 | 64 | 2,763 |
| CA-S-40 | Wadi-El Awag | 1,918 | 76 | 70 | 41,726 |
| CA-S-41 | Wadi-El Nakhl | 551 | 65 | 59 | 3,400 |

(continued)

**Table 5** (continued)

| Catchment no. | Wadi name | Area ($Km^2$) | CN | P100 (mm) | Runoff Vol (1000 $m^3$) |
|---|---|---|---|---|---|
| CA-S-42 | Wadi-El Zaranique | 76 | 65 | 58 | 435 |
| CA-S-43 | Wadi-Araba South' | 65 | 80 | 66 | 1,551 |
| CA-S-44 | Wadi-El Gemal | 284 | 63 | 60 | 1,497 |
| CA-S-45 | Wadi-El Medawara | 67 | 63 | 61 | 353 |
| CA-S-46 | Wadi-El-Malaha North | 66 | 64 | 68 | 572 |
| CA-S-47 | Wadi-Darb El Masaeed | 75 | 63 | 61 | 394 |
| CA-S-48 | Wadi-Sulai | 335 | 79 | 69 | 8,491 |
| CA-S-49 | Wadi-Abou Garph | 74 | 68 | 66 | 839 |
| CA-S-50 | Wadi-Thaman | 156 | 78 | 66 | 3,405 |
| CA-S-51 | Wadi-El Masein | 62 | 73 | 64 | 906 |
| CA-S-52 | Wadi-Beir Abi Hani | 123 | 63 | 63 | 730 |
| CA-S-53 | Wadi-El Raboud | 166 | 82 | 62 | 4,092 |
| CA-S-54 | Wadi-Watir | 3,513 | 78 | 73 | 91,291 |
| CA-S-55 | Wadi-Beir El Kharouba | 1,238 | 64 | 65 | 8,677 |
| CA-S-56 | Wadi-Mukhairet 1 | 75 | 74 | 60 | 1,032 |
| CA-S-57 | Wadi-Dahab | 2,066 | 85 | 76 | 83,634 |
| CA-S-58 | Wadi-Mukhairet 2 | 107 | 76 | 57 | 1,462 |
| CA-S-59 | Wadi-Keid | 1,041 | 81 | 66 | 26,350 |
| CA-S-60 | Wadi-El Aat El Gharbi | 57 | 78 | 54 | 824 |
| CA-S-61 | Wadi-Um Adawi | 362 | 80 | 55 | 6,166 |
| CA-S-62 | Wadi-El Aat El Sharki | 108 | 80 | 51 | 1,501 |
| CA-S-63 | Wadi-Um Tartir | 79 | 73 | 51 | 644 |
| CA-S-64 | Wadi-El Atshan | 98 | 86 | 67 | 3,496 |
| CA-S-65 | Wadi-Al-Garafi | 1,824 | 81 | 90 | 82,129 |
| CA-S-66 | Wadi-Abou-Khadakhed | 369 | 79 | 88 | 14,387 |
| CA-S-67 | Wadi-El Malha | 52 | 85 | 53 | 1,141 |
| CA-S-68 | Wadi-El Abiad | 84 | 84 | 76 | 3,148 |
| CA-S-69 | Wadi-El Harara | 84 | 85 | 77 | 3,411 |

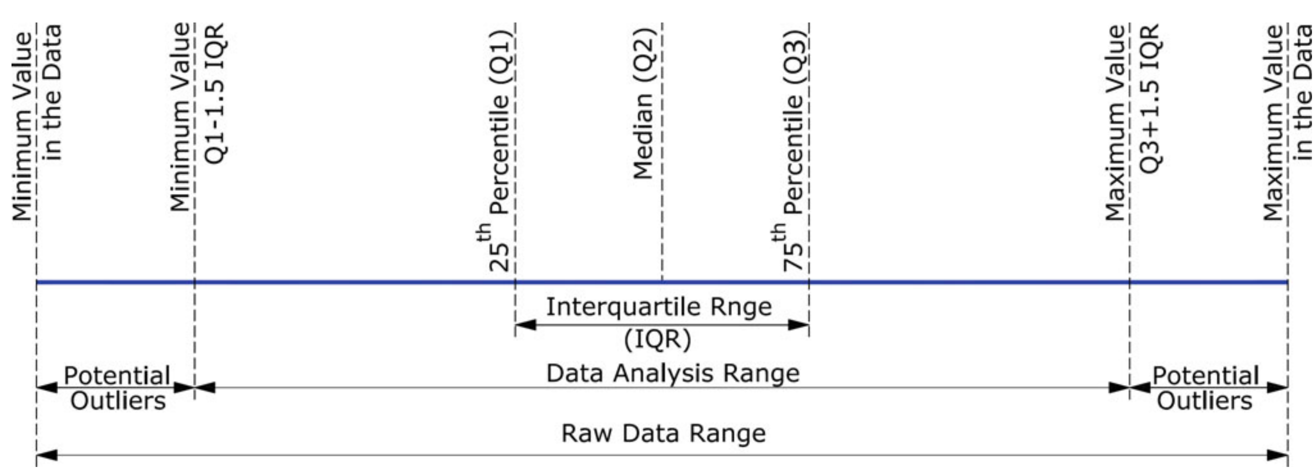


**Fig. 38** Box plot concept

**Table 6** Box plot limits

| Limits | Runoff volume (1000 $m^3$) | Discharge ($m^3$/s) |
|---|---|---|
| *Nile region* | | |
| Q1 | 885 | 15 |
| Q2 | 1399 | 27 |
| Q3 | 3523 | 61 |
| IQR | 2638 | 46 |
| Max limit | 7481 | 130 |
| *Red Sea region* | | |
| Q1 | 1600 | 41 |
| Q2 | 3372 | 110 |
| Q3 | 10828 | 220 |
| IQR | 9228 | 179 |
| Max limit | 24671 | 489 |
| *Sinai region* | | |
| Q1 | 730 | 15 |
| Q2 | 1551 | 42 |
| Q3 | 4092 | 150 |
| IQR | 3362 | 135 |
| Max limit | 9135 | 352 |

## 10 Conclusions

In Egypt, urbanized areas, and associated assets (e.g., agricultural lands, connecting roads, electrical transmission lines) are located at the catchments outfall points in addition to transversal highways. Some of the major and frequent incidents of flooding were recorded with a brief analysis of the causes.

Catchments were delineated using SRTM 90 × 90 DEM data and against versus 1:250,000 topo maps. The threshold for the delineation was set to 50 $km^2$. All morphological catchments' characteristics were extracted using ARC-GIS. Previously generated global Curve Number (CN) shapefile for Egypt was utilized to extract the weighted average CN each catchment. The 1-in-100 maximum daily precipitation from the sparse meteorological station was used to generate an isohyetal map of the study area to obtain the weighted average of 100 years' maximum daily precipitating for each catchment.

SCS method was chosen to calculate the peak discharge and runoff volume. The time of concentration modified from Kirpich equation that combines the effect of the CN was used to obtain the lag time. 6 h SCS type II storm distribution was selected to distribute the 1-in-100 maximum daily precipitation.

The peak discharge and total runoff volume for each catchment were calculated and standardized to calculate Peak Flow Standardized Risk Factor (PFSRF) and Runoff Volume Standardized Risk Factor (RVSRF). Due to the wide range of peak flow and runoff volume, the potential outliers obtained by the quartile technique were ignored during the calculations of the standardized risk factors.

Finally, the catchments were categorized and arranged based on five risk categories (very high, high, moderate, low to moderate, and low) for PFSRF and RVSRF, which prioritize the studies required for flood mitigation measures and show stormwater harvesting potentials.

Two-dimensional HEC-RAS rainfall-runoff model was conducted at Ras-Gharib area using 30 × 30 DEM. The DEM files could not capture the artificial manmade road of Ras-Gharib El-Sheikh-Fadl on the flow directions. The DEM file has been updated based on the available survey data of the road. The flood plain, flow depths, and velocities were obtained, and accordingly, the flood intensities were calculated. The model was verified against aerial photos of the 2016 incident for all stream affecting Ras-Gharib city. The effect of the newly constructed culvert (16 vent 3 m × 3 m) has been checked and the results showed a significant reduction in the flow intensities within the urban areas of Ras-Gharib city.

## 11 Recommendations

- The low-risk catchments cannot be considered as a safe catchment, but it has a lower priority for detailed assessment.
- The treatment of the locations with recorded incidents and providing proper flood mitigation measures are of top priority, even more than the high-risk catchments.
- Based on the runoff volume risk assessment, a priority should be given to stormwater harvesting projects in

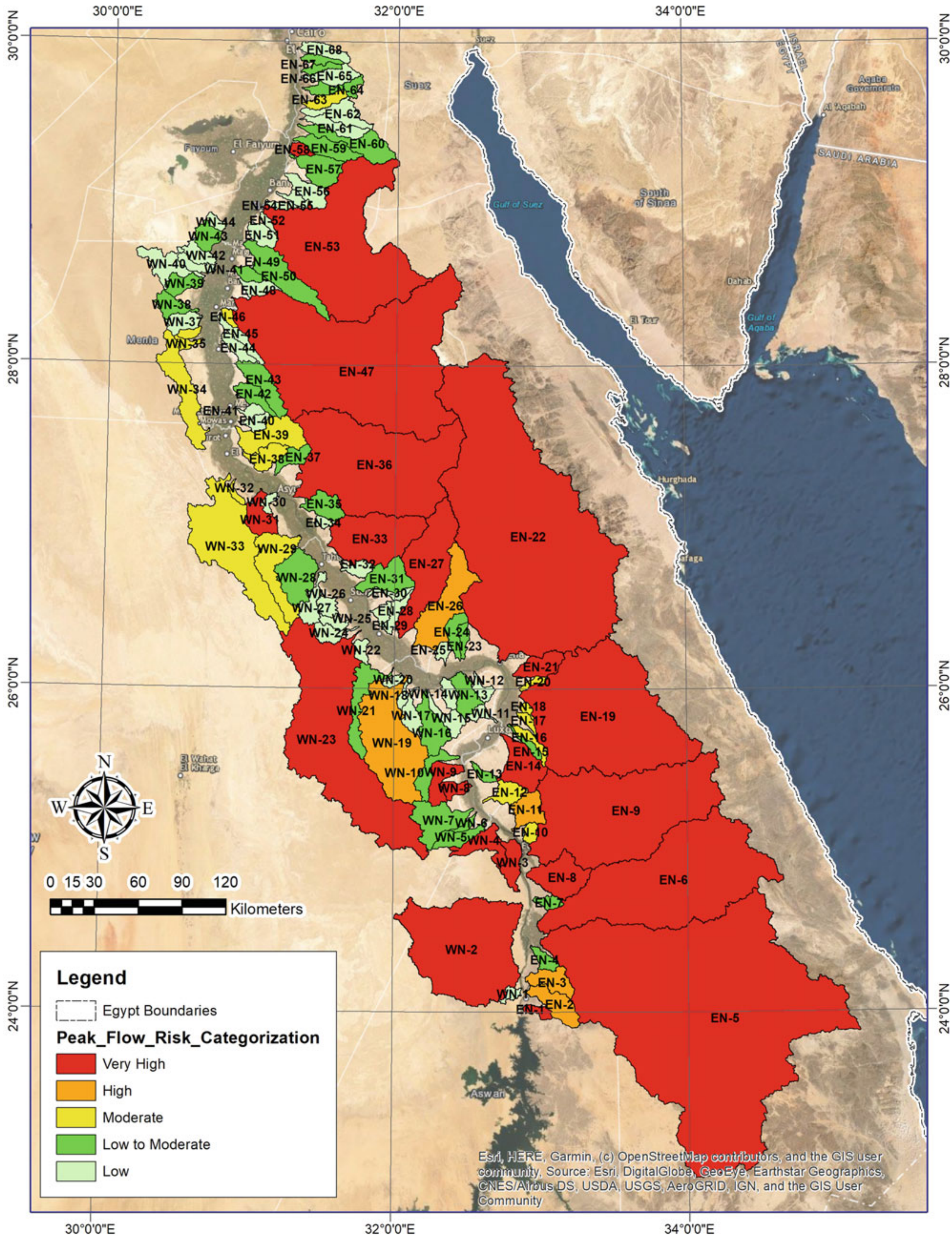


Fig. 39 Nile region catchments categorization as per PFSRF

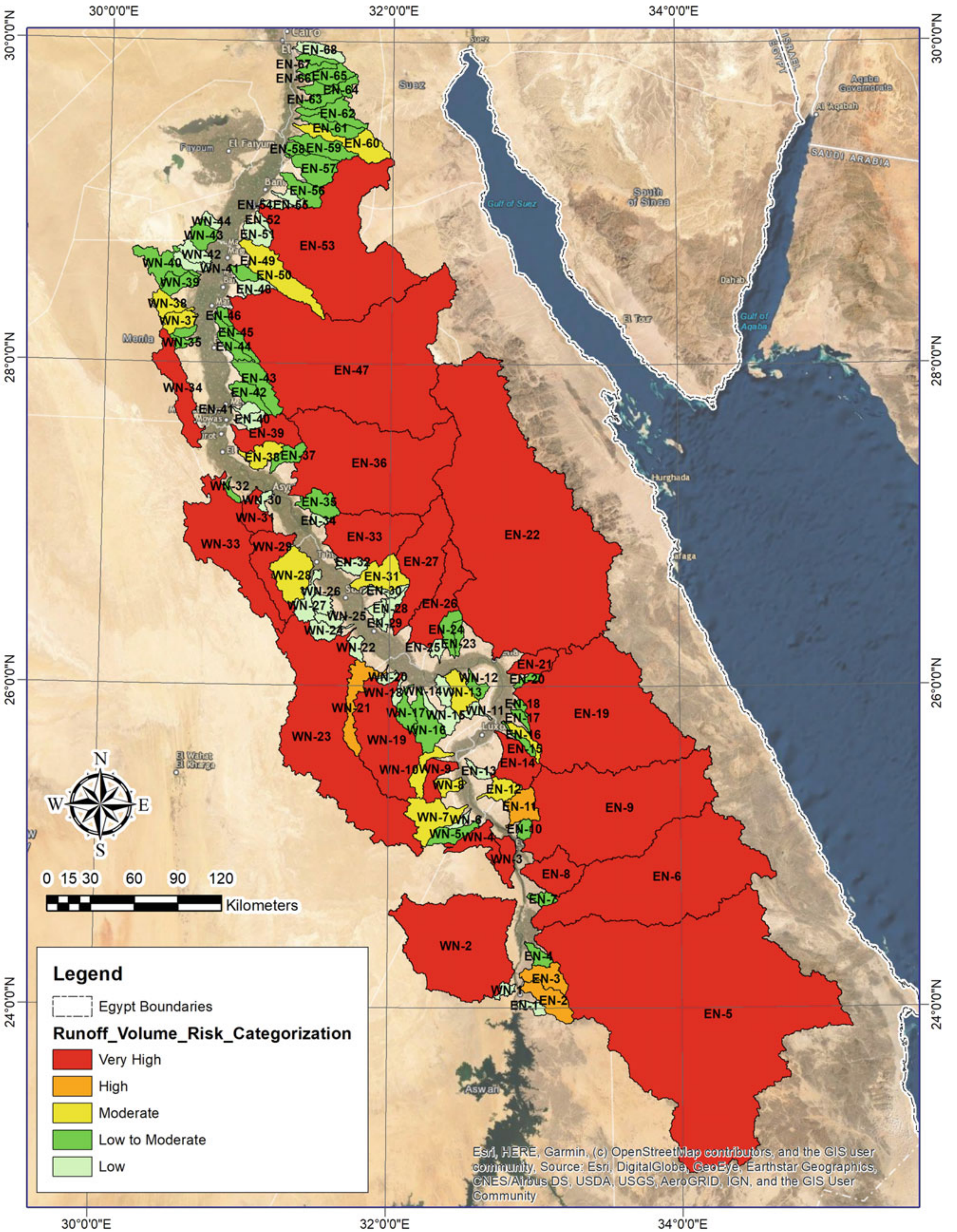


**Fig. 40** Nile region catchments categorization as per RVSRF

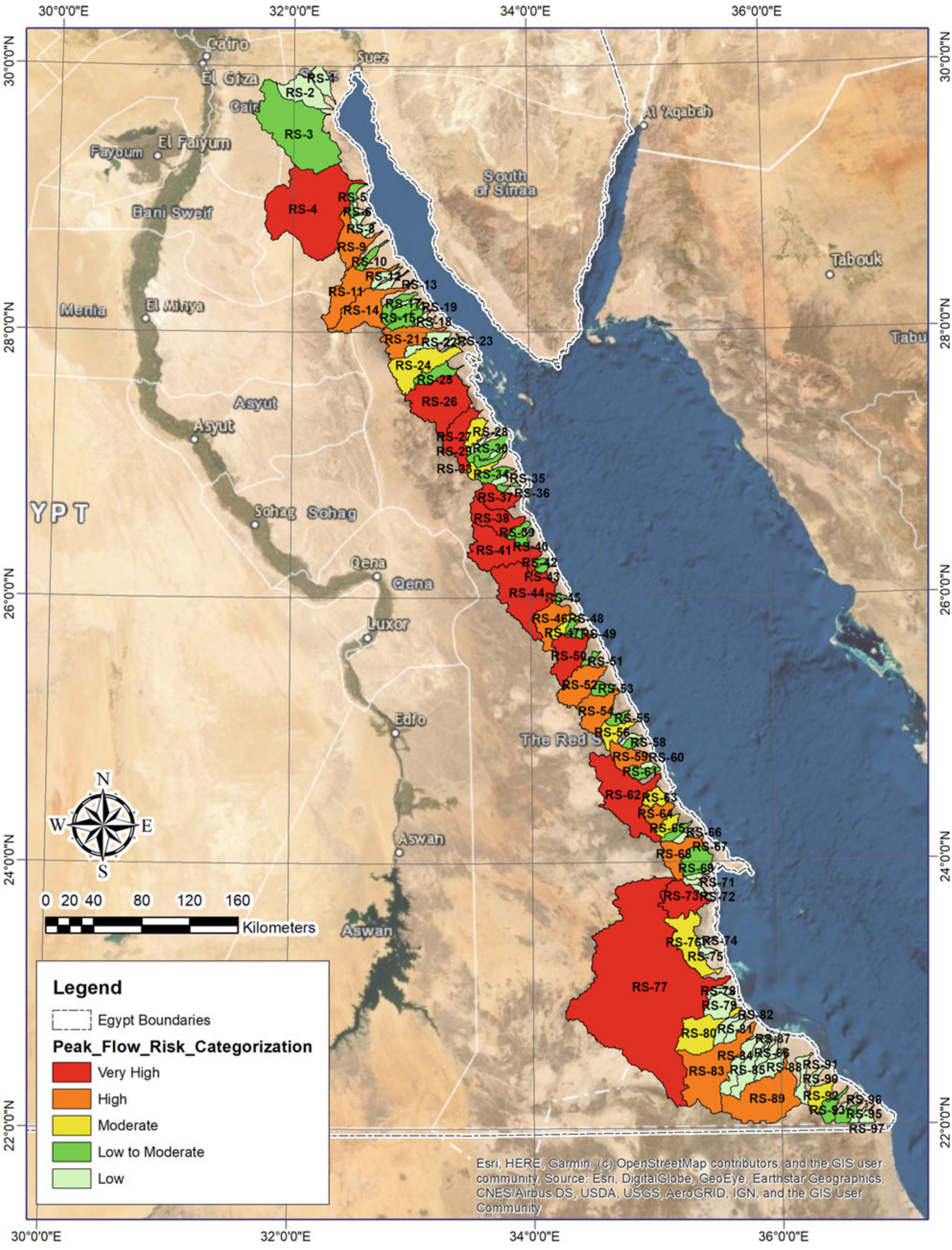


**Fig. 41** Red Sea region catchments categorization as per PFSRF

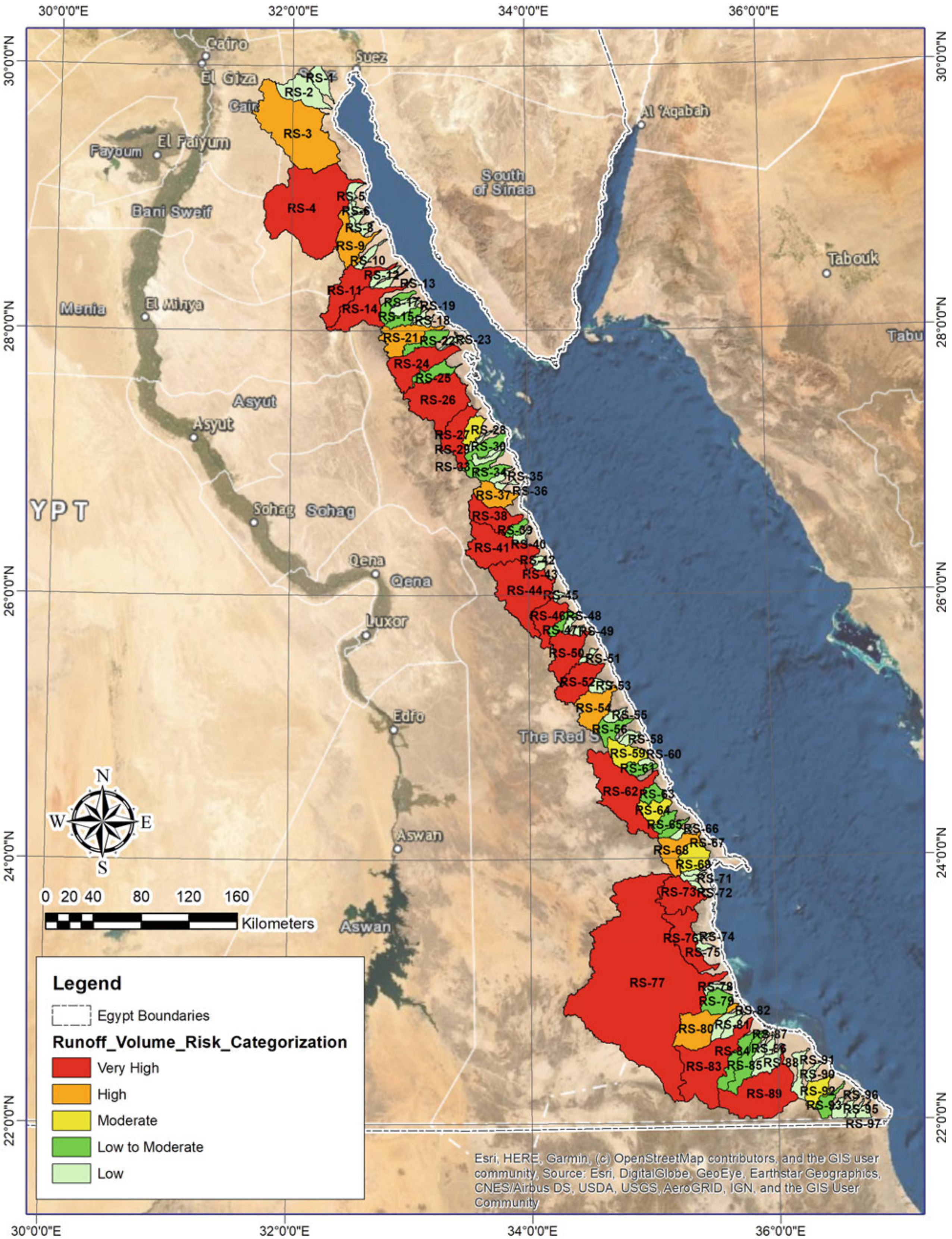


**Fig. 42** Red Sea region catchments categorization as per RVSRF

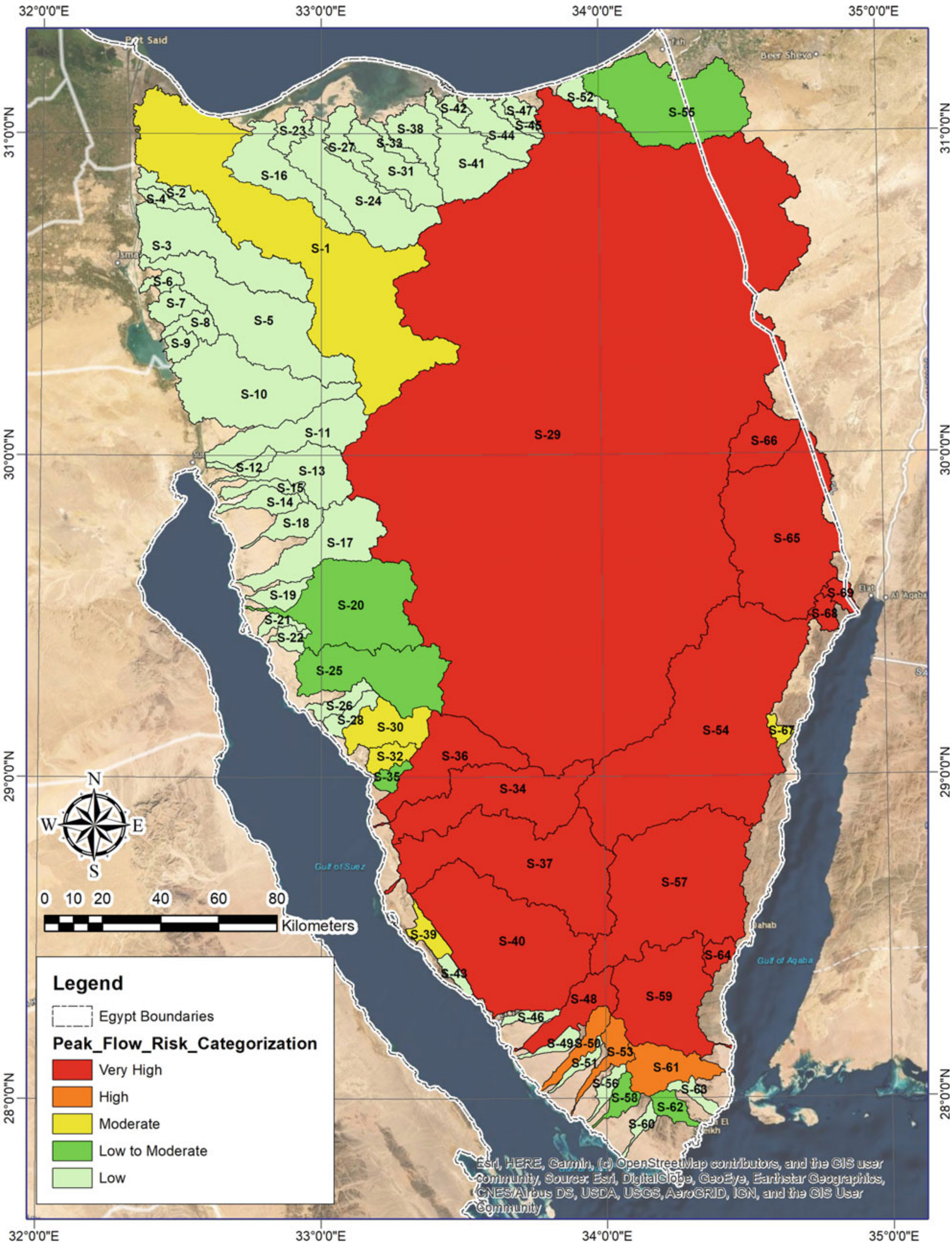


**Fig. 43** Sinai region catchments categorization as per PFSRF

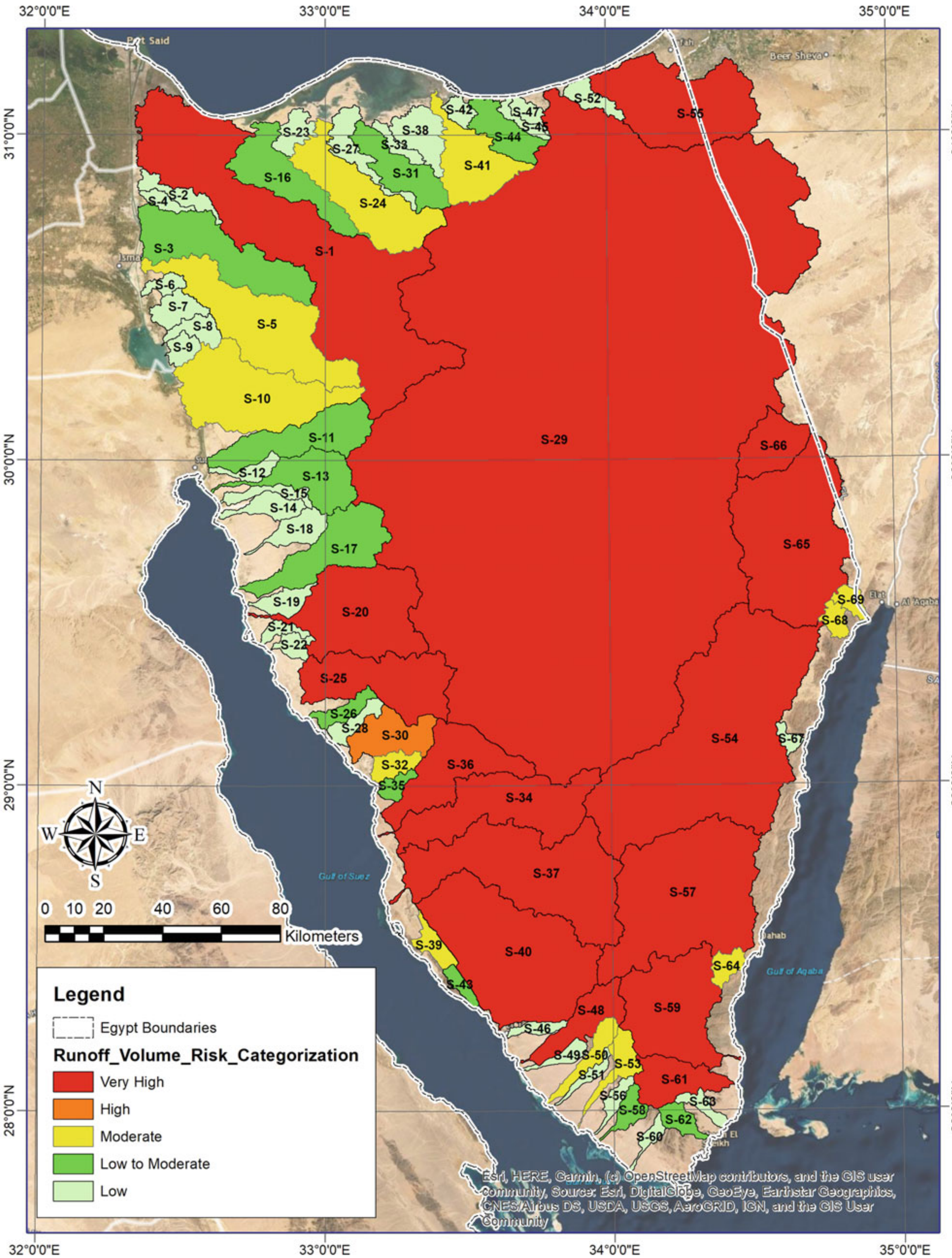


**Fig. 44** Sinai region catchments categorization as per RVSRF

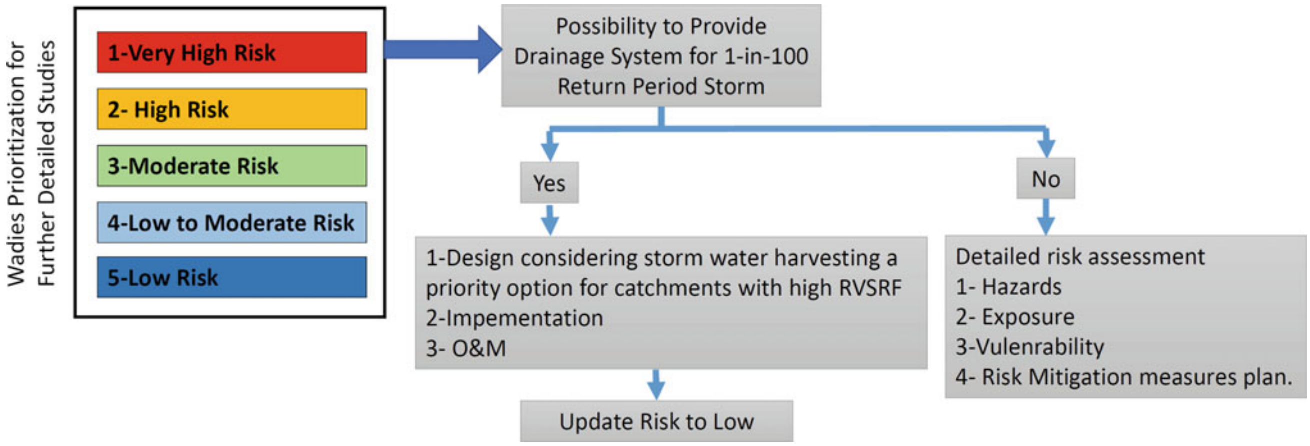


**Fig. 45** Workflow chart for risk assessment


**Fig. 46** Wadi Abou Had catchment on the satellite image

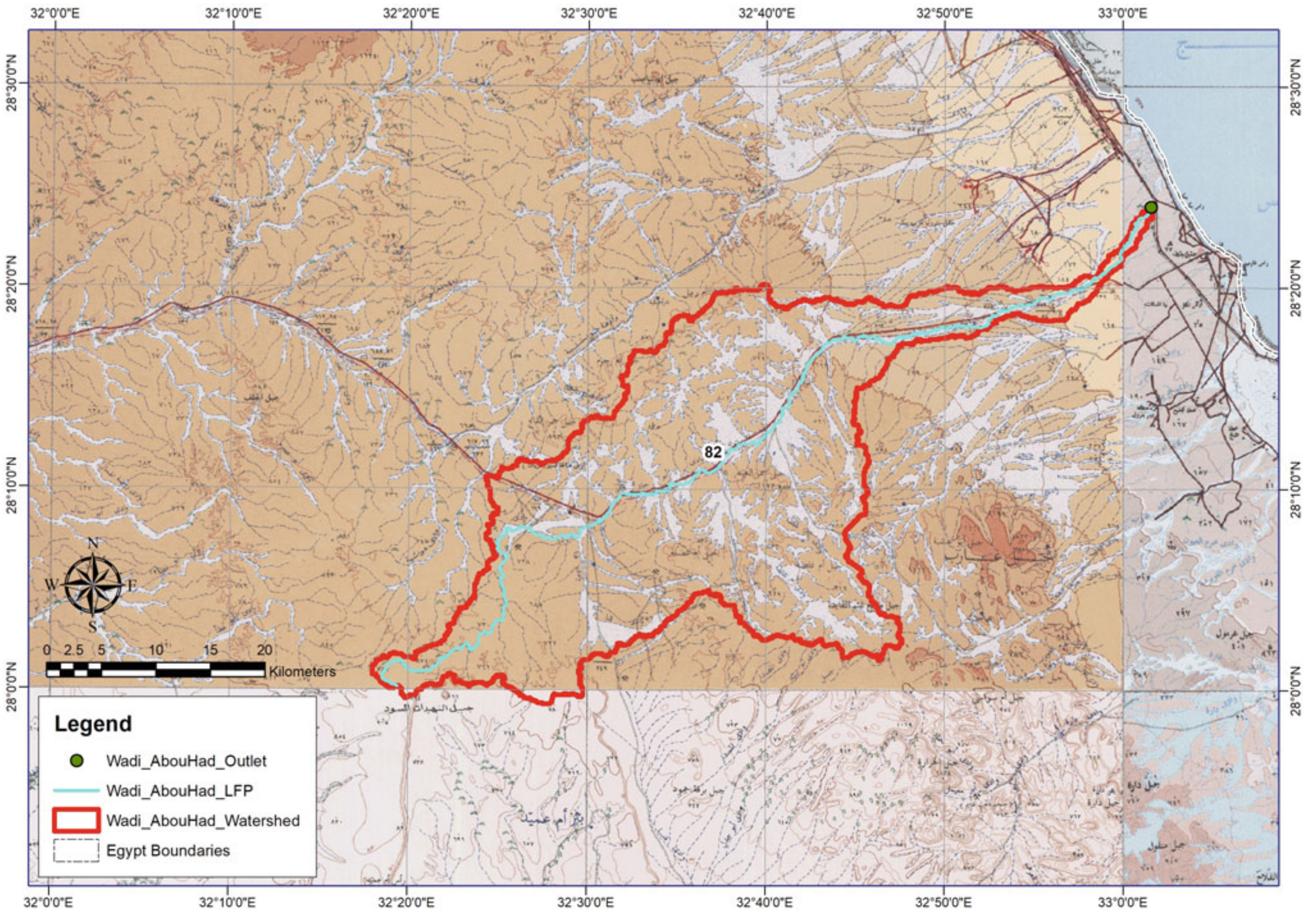


**Fig. 47** Wadi Abou Had catchment on topo maps

order to maximize the return of the investment of flood mitigation measures as a step in solving the freshwater stress in Egypt. The risk of dams' construction should be considered, and the mitigation of providing the dams with spillways designed for a higher return period is mandatory. As a common practice and cost-benefit analysis, the dams' height can be designed to store the 1-in-10 years storm and the spillway design for passing 1-in-200 years' storm.

- Speeding the issuance of the Egyptian code for flood mitigation and storm drainage is a top priority task.
- A committee of the Ministry of Water Resources and Irrigation, Universities irrigation and Hydraulics departments, National Water Research Center, Egyptian Meteorological Authority, National Authority of remote sensing and space science, Water Resources Research Institute, and the National Research Center Department of Geological Science should be formulated. The task of this

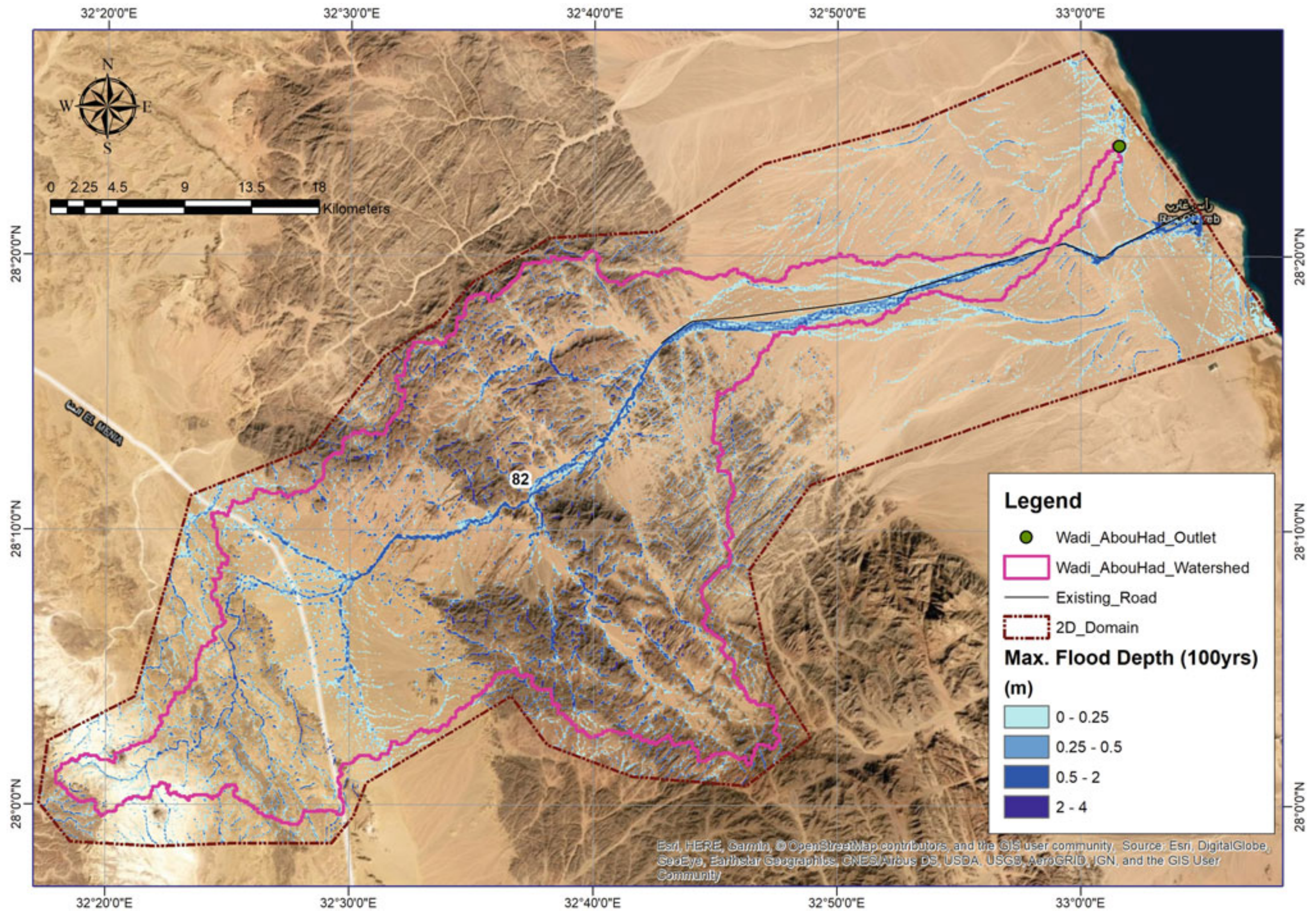


**Fig. 48** HEC-RAS two-dimensional rainfall-runoff model boundaries

committee is to refine tune this study and ensure the latest data availability.

- Reassessment of previously designed flood mitigation measures as per the catchments priorities in light of the Egyptian Code.
- Updating the law and assigning one entity to approve any project hydrological study.
- Updating the law to assure that no permit for any rural road or urbanization extension will be provided without an approved hydrological study.

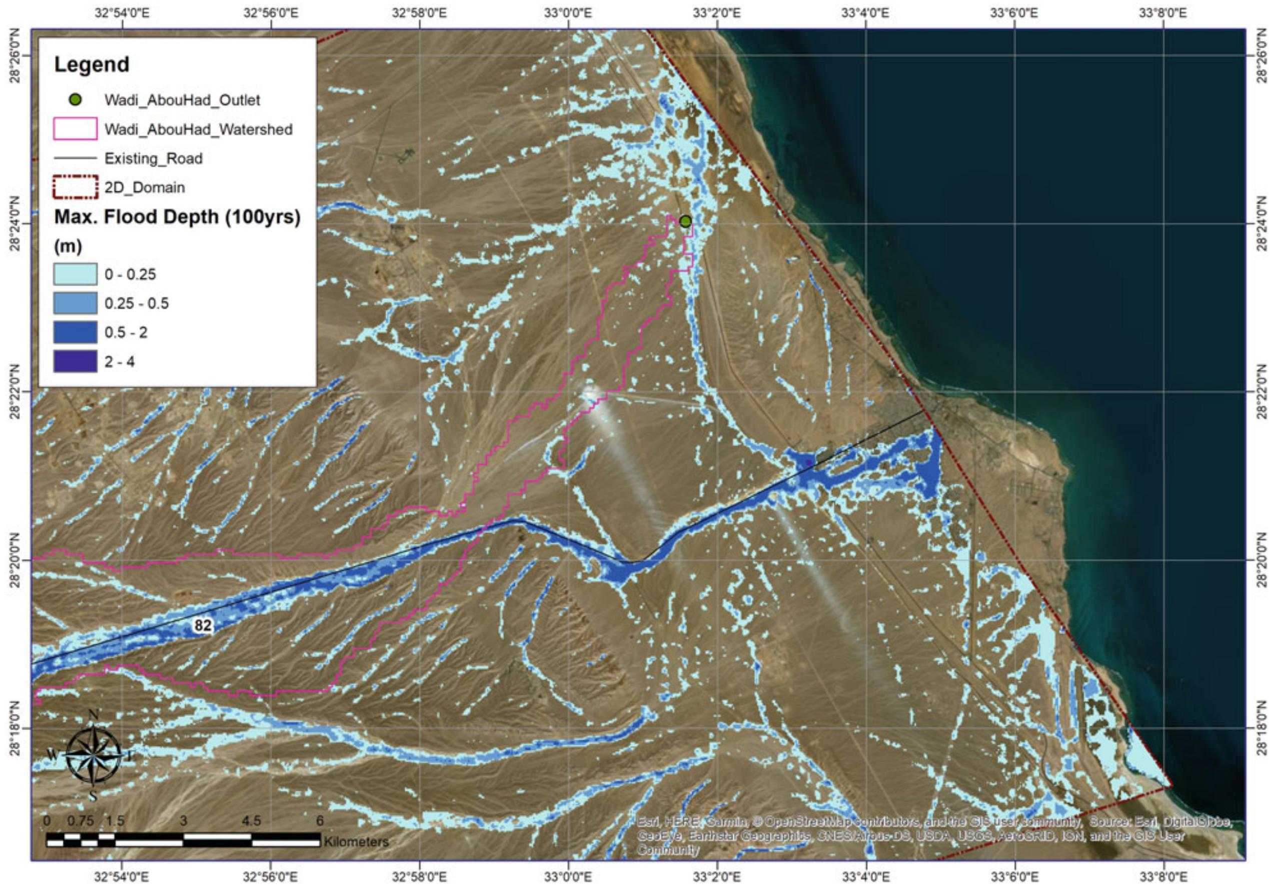


**Fig. 49** 1-in-100 flow depth obtained from HEC-RAS 2D-modeling prior to the construction of flood mitigation measures

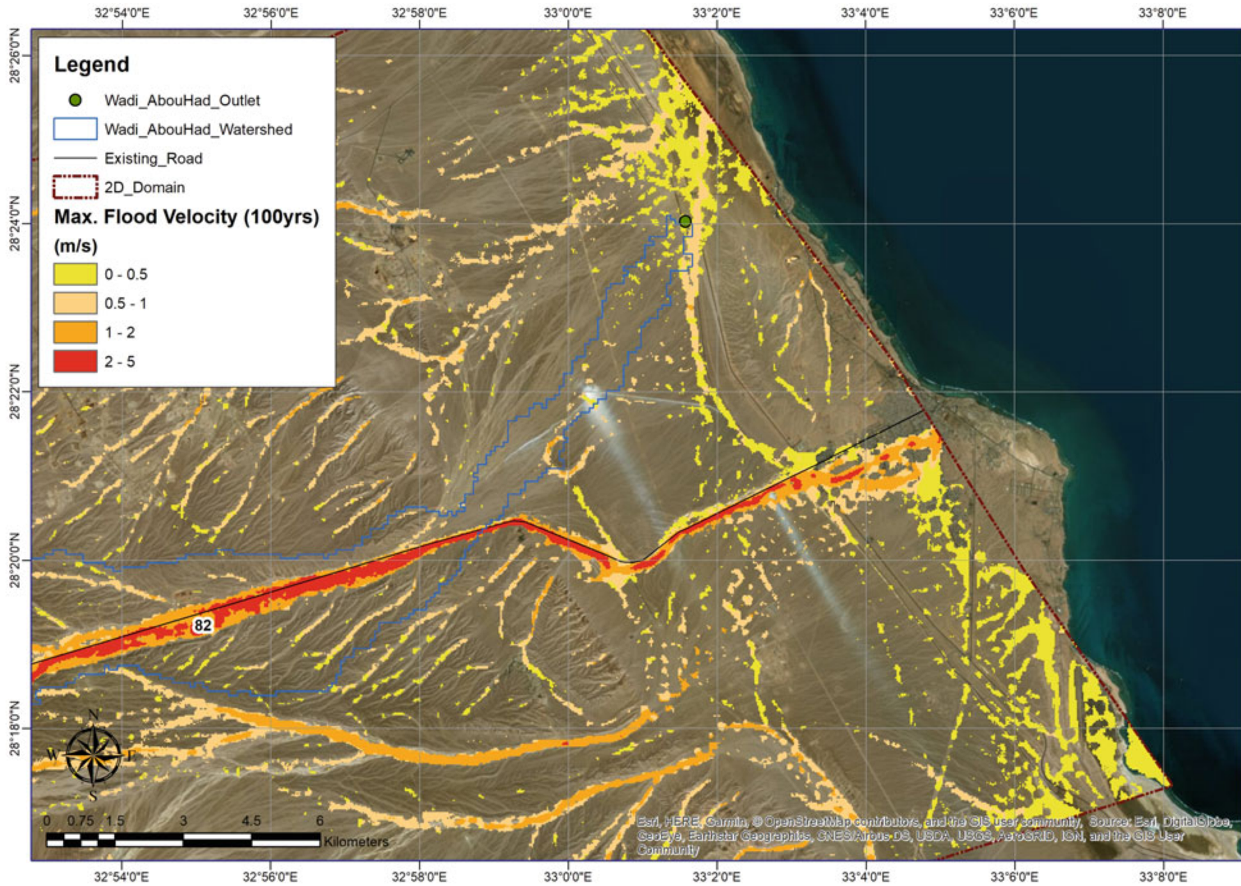


**Fig. 50** 1-in-100 flow velocity obtained from HEC-RAS 2D-modeling prior to the construction of flood mitigation measures

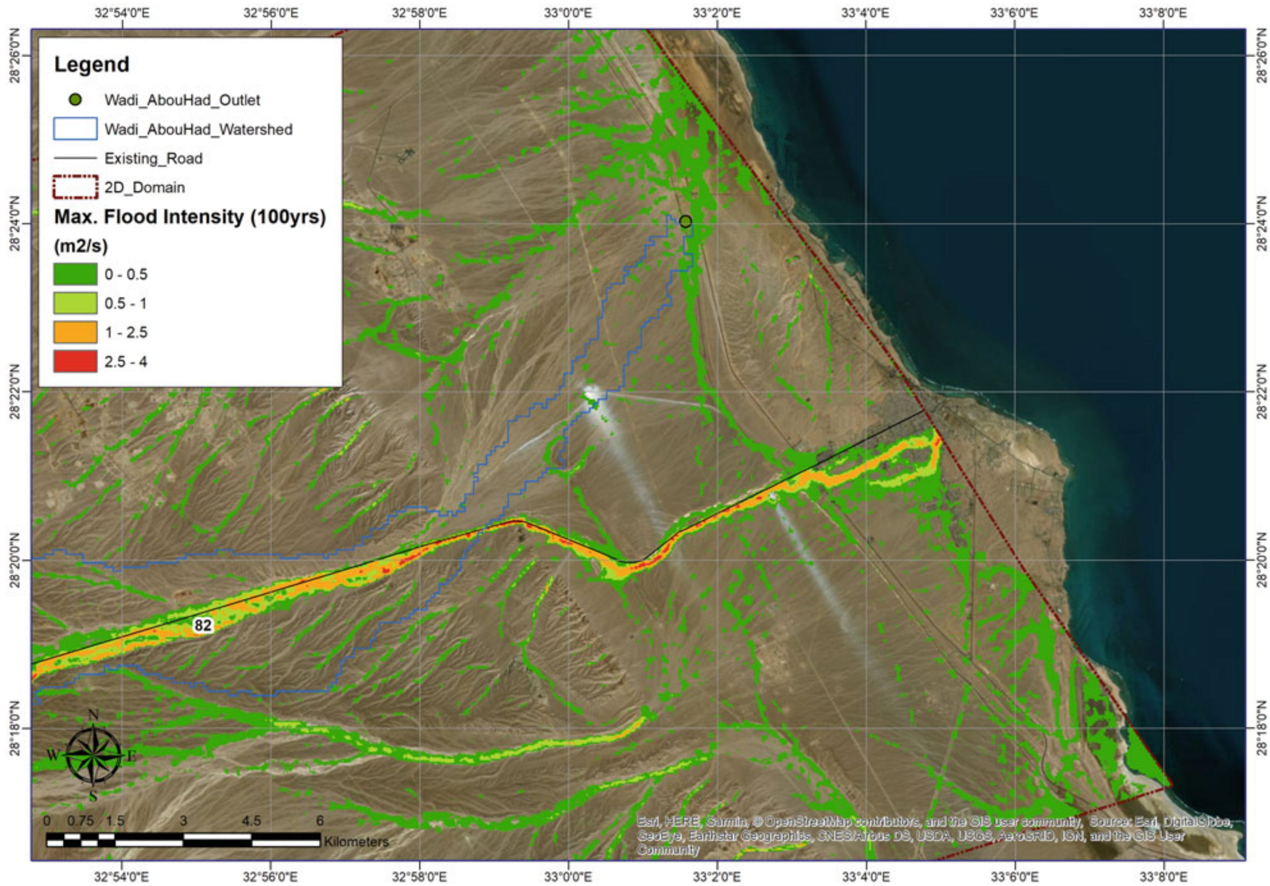


**Fig. 51** 1-in-100 flow Flood intensity from HEC-RAS 2D-modeling prior to the construction of flood mitigation measures


**Fig. 52** **a** Matching water spread at the city entrance, **b** matching flow path inside the city

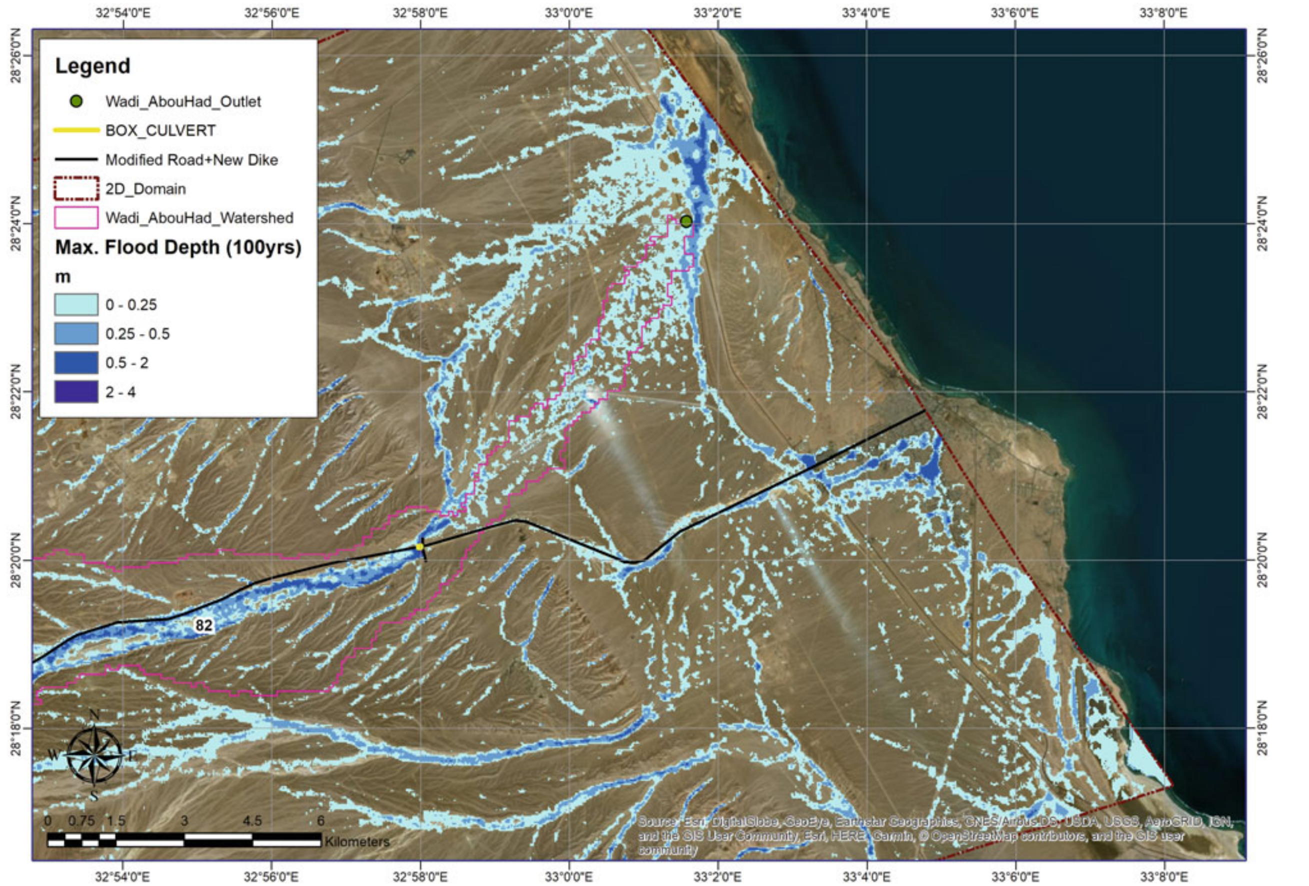


**Fig. 53** 1-in-100 flow depth obtained from HEC-RAS 2D-modeling after the construction of flood mitigation measures

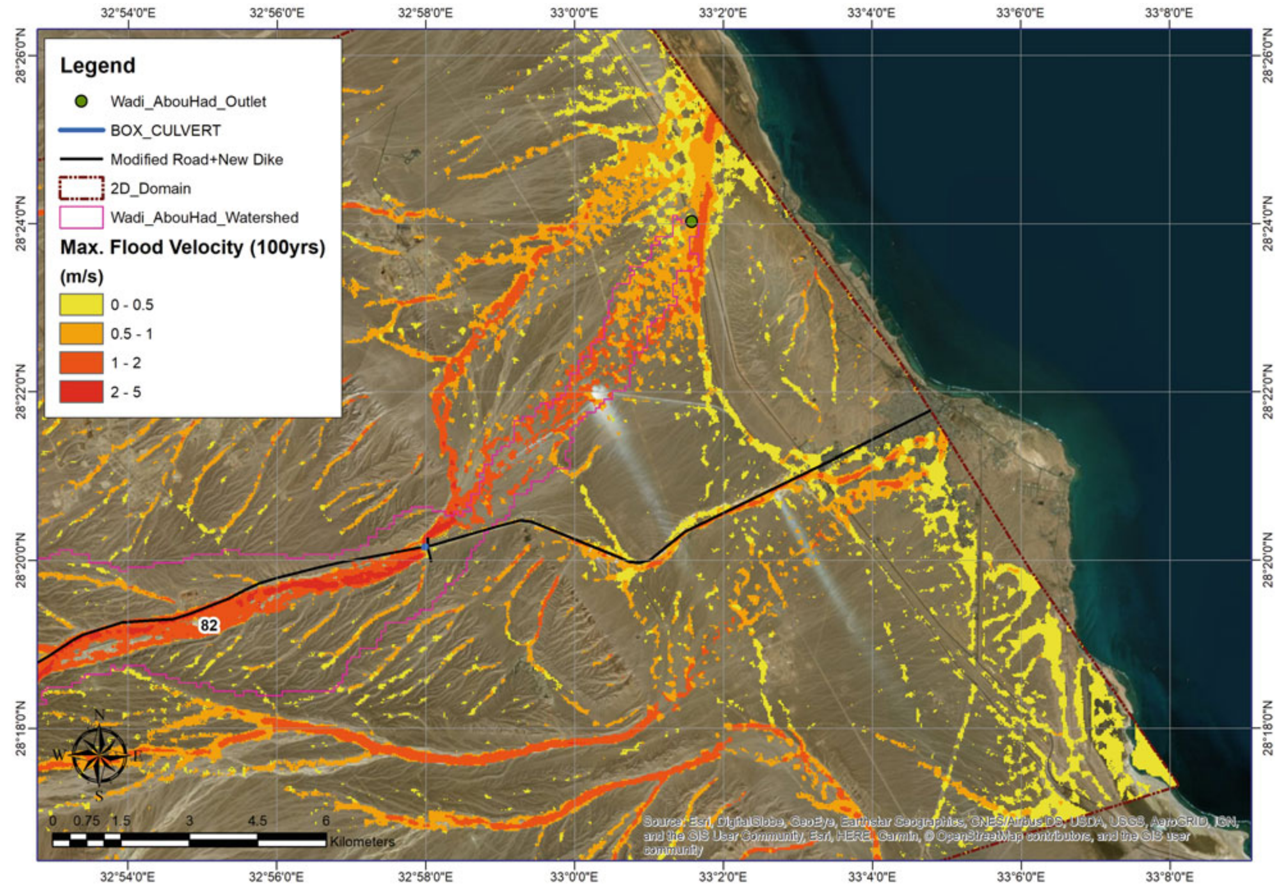


**Fig. 54** 1-in-100 flow velocity obtained from HEC-RAS 2D-modeling after the construction of flood mitigation measures


**Fig. 55** 1-in-100 flow Flood intensity from HEC-RAS 2D-modeling after the construction of flood mitigation measures

## References


Abdalla, F., Shamy, I. El, Bamousa, A. O., Mansour, A., Mohamed, A., Tahoon, M. (2014). Flash floods and groundwater recharge potentials in arid land alluvial basins, Southern Red Sea Coast, Egypt. *International Journal of Geosciences*, *5*, 971–982. https://doi.org/10.4236/ijg.2014.59083.

Abdel-fattah, M., Saber, M., & Kantoush, S. A. (2017). A hydrological and geomorphometric approach to understanding the generation of Wadi flash floods. *Water, 9,* 1–27. https://doi.org/10.3390/w9070553.

Al-Saud, M. (2010). Assessment of flood Hazards of Jeddah Area 2009, Saudi Arabia. *Journal of Water Resource and Protection*. *2*, 839–847. https://doi.org/10.4236/jwarp.2010.29099.

Awadallah, A. G., Saad, H., El-Moustafa, A., & Hassan, A. (2016). Reliability assessment of water structures subject to data scarcity using the SCS-CN model. *Hydrological Sciences Journal, 61,* 696–710. https://doi.org/10.1080/02626667.2015.1027709.

Chow, V. T. (1959). *Open-channel hydraulics*, McGraw-Hill Book Company.

Durrans, S. R. (2007). *Stormwater conveyance modeling and design*. Exton, PA: Bentley Institute Press.

El-Moustafa, A. M. (2012). Weighted normalized risk factor for floods risk assessment. *Ain Shams Engineering Journal, 3,* 327–332. https://doi.org/10.1016/j.asej.2012.04.001.

El-Rayes, A. E., Omran, A. (2009). Flood control and water management in arid environment : Case study on Wadi Hagul, Northwest Gulf of Suez region, Egypt. In *The international on water conservation in arid regions*.

Elsadek, W. M., Ibrahim, M. G., & Mahmod, W. E. (2018). Flash flood risk estimation of Wadi Qena watershed, Egypt using GIS based morphometric analysis. *Applied Environmental Research, 40*, 36–45.

El-Shamy, I. (1992). Recent recharge and flash flooding opportunities in the eastern Desert, Egypt. Annals of geological survey of Egypt. *Annals of the Geological Survey of Egypt, 18,* 323–334.

Eman, M. G., Nigel, W. A., Giles, M. F. (2002). Characterizing the flash flood Hazards potential along the Red Sea Coast of Egypt. In *The Extremes of the Extremes: Extraordinary Floods (IAHS Proceedings & Reports)* (pp. 211–216), Iahs Publication.

European-Commission. (2016). A communication on flood risk management; flood prevention, protection, and mitigation. Retrived June, 20, 19 from http://ec.europa.eu/environment/water/flood_risk/com.htm.

Helmi, A. M., Mahrous, A., Mustafa, A. E. (2019). Urbanization growth effect on hydrological parameters in mega-cities. In *Advances in sustainable and environmental hydrology, hydrogeology, hydrochemistry, and water resources. advances in science, technology & innovation (IEREK interdisciplinary series for sustainable development)*, Springer. https://doi.org/10.1007/978-3-030-01572-5_98.

Horton, R. E. (1945). Erosional development of streams and their Drainage Basins; hydrophysical approach to quantitative morphology. *Bulletin of the Geological Society of America, 56,* 275–370.

Mohamed, M. (2013). Flash flood risk assessment in the eastern desert. M.Sc. thesis, Irrigation, and Hydraulics Department. Ain Shams University.

MWRI. (2016). Ministry of Water Resources and Irrigation Procedures for Rainwater Management.

NASA. (2019). *Socioeconomic data and apllication center. gridded population world (GPW)* (Vol. 4), Retrieved June, 20, 19 from https://sedac.ciesin.columbia.edu/data/set/gpw-v4-population-count-rev11.

Ramirez, J. A. (2000). Prediction and modeling of flood hydrology and hydraulics. In *Inland flood Hazards: Human Riparian and Aquatic communities*, Cambridge University Press.

Rossmiller, R. L. (1980). The rational formula revised. In *International Symposium on Urban Storm Runoff*, University of Kentucky.

Rudari, R. (2017). Flood Hazard and risk assessment. Hazard-Specific Risk Assess. Modul. United Nations Off. Disaster Risk Reduct. 1–16.

Sherman, L. K. (1932). Stream flow from rainfall by the unit graph method. *Engineering News Records, 108,* 501–505.

Sherman, L. K. (1941). The unit hydrograph and its application. *Bull. Assoc. State Eng. Soc., 17,* 4–22.

Syed, T. H., Famiglietti, J. S., Chambers, D. P., Willis, J. K., Hilburn, K. (2010). Satellite-based global-ocean mass balance estimates of interannual variability and emerging trends in continental freshwater discharge. *Proceedings of the National Academy of Sciences of the United States of America*, 1–6. https://doi.org/10.1073/pnas.1003292107.

USAID. (2018). Climate risk profile fact sheet (EGYPT).

USDA. (1986). Urban hydrology for small watersheds (TR-55). United States Department of Agriculture. Natural Resources Conservation Service, Conservation Engineering Division.

Weaver, J. C. (2003). Methods for estimating peak discharges and unit hydrographs for streams in the city of Charlotte and Mecklenburg County. *North Carolina, Water-Resources Investigations Report*. https://doi.org/10.3133/wri20034108.

WMO. (2006). Social aspects and Stakeholder involvement in integrated flood management. APFM Technical Document No. 4, Flood Management Policy Series, Geneva, Switzerland: World Meteorological Organization.

WMO. (2012). Management of flash floods. In *A Tool for Integrated Flood Management, Version 1.0*, WMO/GWP Associated Programme on Flood Management.

Zaid, S. M., Zaghloul, E. S. A., & Ghanem, F. K. (2013). Flashflood impact analysis of Wadi Abu-Hasah on tell El-Amarna archaeological area using GIS and remote sensing. *Australian Journal of Basic and Applied Sciences, 7,* 865–881.